An industrial perspective on metabolic responses of Penicillium chrysogenum to periodic dissolved oxygen feast-famine cycles in a scale-down system

Wang, Xueting; Yang, Qi; Haringa, Cees; Wang, Zejian; Chu, Ju; Zhuang, Yingping; Wang, Guan

DOI
10.1002/bit.28782

Publication date
2024

Document Version
Final published version

Published in
Biotechnology and Bioengineering

Received: 4 February 2024 | Revised: 16 April 2024 | Accepted: 12 June 2024

DOI: 10.1002/bit.28782

ARTICLE

BIOTECHNOLOGY AND BIOENGINEERING WILEY

An industrial perspective on metabolic responses of *Penicillium chrysogenum* to periodic dissolved oxygen feast-famine cycles in a scale-down system

Xueting Wang[1] | Qi Yang[1] | Cees Haringa[2] | Zejian Wang[1] | Ju Chu[1,3] | Yingping Zhuang[1,3] | Guan Wang[1,3]

[1]State Key Laboratory of Bioreactor Engineering, East China University of Science and Technology (ECUST), Shanghai, People's Republic of China

[2]Department of Biotechnology, Delft University of Technology, Delft, The Netherlands

[3]Qingdao Innovation Institute of East China University of Science and Technology, Qingdao, People's Republic of China

Correspondence
Guan Wang, State Key Laboratory of Bioreactor Engineering, East China University of Science and Technology, 130 Meilong Rd, Shanghai 200237, People's Republic of China.
Email: guanwang@ecust.edu.cn

Funding information
National Key Research and Development Program of China, Grant/Award Number: 2021YFC2101000; Natural Science Foundation of Shanghai, Grant/Award Number: 19ZR1413600; Fundamental Research Funds for the Central Universities, Grant/Award Number: JKF01221709; National Natural Science Foundation of China, Grant/Award Numbers: 31900073, 21978085

Abstract

While traveling through different zones in large-scale bioreactors, microbes are most likely subjected to fluctuating dissolved oxygen (DO) conditions at the timescales of global circulation time. In this study, to mimic industrial-scale spatial DO gradients, we present a scale-down setup based on dynamic feast/famine regime (150 s) that leads to repetitive cycles with rapid changes in DO availability in glucose-limited chemostat cultures of *Penicillium chrysogenum*. Such DO feast/famine regime induced a stable and repetitive pattern with a reproducible metabolic response in time, and the dynamic response of intracellular metabolites featured specific differences in terms of both coverage and magnitude in comparison to other dynamic conditions, for example, substrate feast/famine cycles. Remarkably, intracellular sugar polyols were considerably increased as the hallmark metabolites along with a dynamic and higher redox state nicotinamide adenine dinucleotide hydrogen/nicotinamide adenine dinucleotide of the cytosol. Despite the increased availability of NADPH for penicillin production under the oscillatory DO conditions, this positive effect may be counteracted by the decreased adenosine triphosphate supply. Moreover, it is interesting to note that not only the penicillin productivity was reduced under such oscillating DO conditions, but also that of the unrecyclable byproduct ortho-hydroxyphenyl acetic acid and degeneration of penicillin productivity. Furthermore, dynamic flux profiles showed the most pronounced variations in central carbon metabolism, amino acid (AA) metabolism, energy metabolism and fatty acid metabolism upon the DO oscillation. Taken together, the metabolic responses of *P. chrysogenum* to DO gradients reported here are important for elucidating metabolic regulation mechanisms, improving bioreactor design and scale-up procedures as well as for constructing robust cell strains to cope with heterogenous industrial culture conditions.

KEYWORDS
dissolved oxygen, flux analysis, industrial, metabolomics, *Penicillium chrysogenum*, scale down

Xueting Wang and Qi Yang are contributed equally to this study.

1 | INTRODUCTION

During bioprocess development, the so-called scale-up effect often leads to reduced production performance by 10–30% in terms of titer, rate and yield (T. R. Y.), and in some cases, even batch failures (Kampers et al., 2021). This is most likely related to a reduction of the mixing intensity and a decrease in the mass transfer capacity upon bioreactor scaling-up from small to large scale (Wang et al., 2015). Generally, intracellular metabolic reaction times do not scale with the bioreactor size, having timescales in the order of (tens of) seconds, while mixing times in large-scale bioreactors (2–150 m^3) can reach 10–300 s in stirred tank reactors (STR) and bubble columns used in microbial processes and much higher (10–3000 s) in reactors for plant and animal cells (Wang, Haringa, Tang, et al., 2020). This timescale difference inevitably leads to the generation of various concentration gradients within the bioreactor, such as substrate, DO, temperature, and pH gradients (Lara, Galindo, et al., 2006; Nadal-Rey et al., 2021). As a consequence, differences in the environment experienced by the cells may change the biomass growth and production performance. Whether these concentration gradients will have a considerable effect on the cellular performance depends on many factors, the most important of which are the gradient magnitude and the frequency at which the cells are exposed to such gradients (Paul et al., 2020; Yang et al., 2007). For example, as for the substrate, the former depends on the feed concentration and the feed point relative to the location of the impeller in the bioreactor while the latter depends on the global circulation time of the bioreactor under cultivation conditions (Neubauer & Junne, 2016).

To investigate the physiological response of microorganisms exposed to heterogeneous environments for long periods of time, a scale-down approach was proposed to simulate the dynamic microenvironment experienced by the cells at large scale (Neubauer & Junne, 2010; Wang et al., 2014). Information derived from scale-down studies can be used to improve scale-up procedures and to evaluate or identify problems at the production level. Among these formed nonhomogeneous environmental factors, fluctuations of substrate and DO concentration are the main factors affecting cell growth and product formation (Kuschel & Takors, 2020). To the best of our knowledge, there have been many scale-down studies on substrate concentration gradients that dealt with various industrial cell factories, and these studies have provided valuable insights into cellular metabolism and suggestions for process intensification (de Jonge et al., 2011; Liu, Wang, et al., 2021; Suarez-Mendez et al., 2017; Vasilakou et al., 2020; Wang et al., 2019; Wang, Zhao, et al., 2018). Although substrate gradients mostly result in performance loss, several interesting studies have demonstrated that substrate gradients can contribute to desired fungal morphology and result in a substantial increase of the productivities (Bhargava, Nandakumar, et al., 2003; Bhargava et al., 2003a, 2003b). Hence, such uncertainty about the performance of the production organism in the full-scale bioreactor imperils the competitiveness of bioprocesses (Takors, 2012). Yet, the influence of oxygen as substrate is often left aside with the assumption of sufficient DO levels in the entire bioreactor (Haringa et al., 2016). In reality, oxygen transfer takes place throughout the aerated broth, and the manifestation of oxygen gradients is a complex interplay between local mass transfer (Garcia-Ochoa & Gomez, 2009), mixing, consumption and significant differences in local solubility due to hydrostatic pressure gradients.

In spite of its importance, only very scarce reports have determined the effects of DO gradients on overall productivity and product quality at the molecular level. Among such few exceptions, for example, to investigate the effect of DO heterogeneity on plasmid DNA produced by *Escherichia coli*, DO gradients were simulated and dynamic flux balance analysis showed intermittent changes in metabolic fluxes and cytochromes activities. More interestingly, their results suggest that heterogeneous oxygen availability affects the titer and topology but not the fidelity of plasmid DNA. This should be considered during bioreactor operation at several scales and for better strain and vector design (Jaén et al., 2017). Lara, Leal, et al. (2006) first used a two-compartment scale-down system consisting of the anaerobic (0% DO, residence time, 33 s) and aerobic (10% DO, residence time, 17 s) vessels whereupon cells were continuously circulated in between to mimic DO gradients imposed on *E. coli*, expressing recombinant green fluorescent protein. Their results showed that transcription levels of mixed acid fermentation genes (*ldhA*, *poxB*, *frdD*, *ackA*, *adhE*, *pflD*, and *fdhF*) under oscillatory DO conditions increased between 1.5 to over sixfold compared to the control (constant 10% DO); it was found that *E. coli* was more inclined to express high-affinity but less energy-efficient cytochromes under DO fluctuation conditions. In addition, under such oscillating DO conditions *E. coli* preferentially employs tricarboxylic acid (TCA) cycle as two separate branches, and thus presents a behavior typical of anaerobic cultures. Likewise, Anane et al. (2021) used a two-compartment system comprising a stirred reactor (STR) and a plug flow reactor (PFR) wherein CHO cells expressing a recombinant protein was subjected to DO gradients alongside the PFR at varying residence time from 70 to 120 s. The results showed that when the cell residence time in the PFR was above than 90 s, a 15% decrease in live cell density and significant lactate accumulation occurred in the stationary phase. Interestingly, the recombinant protein productivity was not affected by the DO gradients, although the purity of the product was adversely affected. Aside from utilizing multiple reactors, DO gradients can also be simulated by setting a fluctuating on/off supply of air in a one-compartment scale-down system. For example, Sweere et al. (1988) investigated the influence of a periodically changing oxygen concentration on the growth of baker's yeast in a continuous culture. Their results showed that cells experiencing rapid fluctuations between limited oxygen and unlimited oxygen with a frequency of 1 or 2 min^{-1} significantly led to reduced biomass growth, increased byproduct formation and enhanced oxygen demands. However, the RNA, protein and carbohydrate contents of the cells exposed to the DO fluctuations did not differ significantly from those in cells from an oxygen-unlimited or an oxygen-limited culture. Nonetheless, some cases showed that the application of oxygen-limiting conditions leads

to a considerable increase in protein specific productivity (Garcia-Ortega et al., 2017; Lu et al., 2018; Pedersen et al., 2012).

For industrial-scale production of penicillin with the filamentous fungus *Penicillium chrysogenum*, oxygen is required for cellular growth, maintenance and also as the co-substrate for the isopenicillin synthetase (IPNS) in the second step of the penicillin biosynthetic pathway (White et al., 1982). Nevertheless, few studies have reported the DO profiles in the industrial-scale bioreactor and little has been known about the effect of DO on cellular physiology during penicillin fermentation with *P. chrysogenum*. To the best of our knowledge, earlier studies only involved the analysis of macroscopic metabolic differences and did not deeply analyze the metabolic regulation under DO fluctuation conditions, and also did not consider the real fluctuating environment experienced by microorganisms in large-scale bioreactors. For example, Vardar and Lilly (1982) first investigated the effects of periodic fluctuations in DO levels on penicillin production and the respiratory metabolism in *P. chrysogenum*. Their results revealed that the rates of oxygen uptake and penicillin production decreased sharply at DO concentrations below 0.019 and 0.082 mol/m^3, respectively, suggesting that DO concentrations affecting cellular respiration and product formation differ. In addition, the production of penicillin was restored by adjusting the DO back to above the critical oxygen concentration. Henriksen et al. (1997) also reported that cellular respiration was unaffected and penicillin production decreased at a DO concentration of 0.019 mol/m^3. Larsson and Enfors (1988) constructed a two-compartment fermentor system consisting of one well-mixed STR and one minor anaerobic PFR based on which *P. chrysogenum* cells were circulated in between. Their results showed that a circulation time of above 5 min in the PFR and with a volume of 6% of the STR caused irreversible effects on the respiration of *P. chrysogenum*. Nevertheless, the cellular mechanisms relating these phenomena to changes in productivity have not been revealed in these previous studies. In addition to this, there were certain limitations in previous experimental design, such as the use of pressure cycling fluctuations to achieve DO fluctuations. Under the same pressure and temperature setting, CO_2 solubility in the fermentation broth was 25–30 times higher than oxygen solubility, which may directly lead to a more substantial cyclic fluctuation of CO_2 concentration in the bioreactor. Moreover, most of their studies used the batch or fed-batch fermentation mode, which was accompanied by changes in biomass concentration, product concentration and even limiting factors. To address this, such experiments should be performed as steady-state continuous cultivations via manipulating the inlet gas composition only, thus keeping all other culture parameters constant. Until recently, we for the first time investigated the response of glucose-limited chemostat cultures of an industrial *P. chrysogenum* strain to different DO levels under both DO shift-down (60% → 20%, 10% and 5%) and DO ramp-down (60% → 0% in 24 h) conditions (Yang et al., 2022). The results showed that the penicillin productivity was reduced by 25% at a DO value of 5% under steady state conditions while only a 14% reduction in penicillin productivity was observed as the DO level was ramped down to 0%. In addition, flux balance analysis suggested that the glyoxylate shunt was significantly enhanced to facilitate the maintenance of intracellular redox state when the DO level was below 20%. Nonetheless, most previous scale-down studies did not take relevant industrial-scale flow field conditions into account, but rather only a limited set, and some are more worst-case scenarios (Wang, Haringa, Noorman, et al., 2020).

Large-scale bioreactors for penicillin production can nowadays reach 300 m^3 or larger in volume (de Jonge et al., 2011). As the bioreactor dimension increases, due to poor mixing and mass transfer limitations in industrial-scale bioreactors as well as high cellular metabolic activities, spatial DO concentration gradients, that is zones with low DO near the substrate feeding point and zones with high DO near the sparger at the bottom. Consequently, cells are periodically exposed to an oscillating DO gradient environment that can affect their metabolic behavior, which can eventually contribute to the different production performance generally observed between large-scale cultures and laboratory-scale studies. For example, in a 100 m^3 penicillin production vessel, the registered DO in the bottom, with a minimum of 0.18 mol/m^3 during the fed-batch fermentation, which indicated there might be a much lower DO in the upper layer, farther away from gas inlet and with a much lower hydrostatic pressure (Goldrick et al., 2015). In a comparable 150 m^3 penicillin production reactor, the DO in the lower fermentation broth was twice as high as in the upper layer, and at the end of fermentation, the DO concentration in the upper fermentation broth was below 0.05 mol/m^3 (Haringa et al., 2016). It has been shown that the mixing time of filamentous fungal fermentation broth is about 1 to a few minutes for reactors with working volumes of 50 m^3 and above (Pollard et al., 2007). For instance, mixing experiments have been performed with aerated and nonaerated water and broth as working fluids in a 54 m^3 penicillin fermentor by royal DSM, and the experimental results showed that the circulation time under aerated and nonaerated broth conditions was about 30 and 80 s, respectively (Haringa et al., 2016). However, to our knowledge, only very scarce reports have determined the effects of industrial-relevant DO gradients on microbial growth and product formation. Among such few exceptions are the recent study of periodic DO fluctuations in one-compartment scale-down system for determining the effect of *P. chrysogenum* growth and penicillin productivity (Janoska et al., 2022). However, they did not fully explore key intracellular mechanisms associated with cell growth and product formation, which requires an in-depth investigation of intracellular metabolite dynamics and dynamic flux responses under such industrial-relevant conditions.

In this study, we aimed to investigate the effect of industrial-relevant oscillatory DO on the in vivo kinetics of central metabolite pools and dynamic flux responses in a high-producing strain of *P. chrysogenum*. Scale-down experiments were performed as glucose-limited chemostat cultures were subjected to DO fluctuations by setting a fluctuating on/off supply of nitrogen and oxygen only in a one STR system. To our knowledge, this is the first report that incorporates in a single study information on penicillin production, byproduct formation, metabolite pools and flux response of *P. chrysogenum* to highly dynamic, industrial-relevant, DO fluctuation

conditions. The results obtained are useful for understanding the metabolic response of *P. chrysogenum* to oscillatory DO environments typically observed in industrial-scale bioreactors.

2 | MATERIALS AND METHODS

2.1 | Strain

The *P. chrysogenum* Wisconsin 54−1255 was purchased from ATCC, and fungal spores were prepared on potato dextrose agar (PDA) medium, and the concentrated spore suspensions were aliquoted and stored in aqueous glycerol solution (30% [v/v] glycerol in demineralized water) at −80°C. Spore suspension inoculation was used in all experiments and were prepared to ensure that the final spore concentration in the bioreactor after the inoculation was about 1×10^6/mL, as described previously (Wang et al., 2019).

2.2 | Cultivation media

The composition of the medium for the batch phase and chemostat cultivation is the same, containing (g/kg): 16.5 g $C_6H_{12}O_6{\cdot}H_2O$, 5 g $(NH_4)_2SO_4$, 1 g KH_2PO_4, 0.5 g $MgSO_4{\cdot}7H_2O$, 2 mL trace elements, 1 mL antifoaming agent. The trace element composition (per kg of deionized water) was 75 g $Na_2EDTA{\cdot}2H_2O$, 10 g $ZnSO_4{\cdot}7H_2O$, 10 g $MnSO_4{\cdot}1H_2O$, 20 g $FeSO_4{\cdot}7H_2O$, 2.5 g $CaCl_2{\cdot}2H_2O$, 2.5 g $CuSO_4{\cdot}5H_2O$. The phenylacetic acid (PAA) concentrations in the batch and the chemostat media were supplied at 0.4085 and 0.68 g/kg, respectively, which was neither limiting nor toxic to cell growth throughout the cultivation (Douma et al., 2012). The preparation and sterilization of the cultivation medium have been described previously (Douma et al., 2010). Briefly, glucose solution and the PAA-containing salt solution were prepared and sterilized at 110°C and 121°C for 40 and 30 min, respectively. The PAA was dissolved in a KOH solution, with a PAA: KOH molar ratio of 1:1.2 (Wang et al., 2021).

2.3 | Chemostat cultivation

For all experiments, glucose-limited chemostats with a working volume of 3 L were carried out in a 5 L turbine stirred bioreactor (Shanghai Guoqiang Bioengineering Equipment Co., Ltd.) at a dilution rate of 0.05 h^{-1}. When the glucose in the batch phase was depleted, the culture was switched to chemostat mode. The broth was drained by a peristaltic pump through an overflow tube located at the bioreactor gas/liquid interface. The DO level was detected with an oxygen probe (Visiferm DO HAMILTON), which was calibrated at 100% at 0.4 bar overpressure (dissolved oxygen [DO] approx. 0.3 mol/m^3). The temperature was maintained at 25°C, the airflow rate was set at 2 L/min, the stirrer speed was set at 600 rpm and pH was controlled at 6.5 with 4 M sodium hydroxide using a sterilizable pH probe (Mettler-Toledo). The off-gas oxygen and carbon dioxide fractions were monitored in real-time using an off-gas mass spectrometer (Prima BT, Thermo Fisher Scientific).

2.4 | Experimental design for fast DO "feast/famine" cycles

To investigate the metabolic response of *P. chrysogenum* cells in response to the fluctuating DO environment occurring in large-scale fermentation, we propose a scale-down setup to mimic the periodic fluctuations of DO, that is, DO fluctuating cycles, at the laboratory-scale bioreactor. Periodic DO fluctuation experiments were performed on the basis of the glucose-limited chemostat culture at a dilution rate of 0.05 h^{-1}, thus keeping all the other parameters constant during the cultivation process. After extracellular glucose was depleted in the batch phase, continuous cultivation was immediately initiated. Steady state was achieved after 120 h (six residence times) cultivation, and then DO fluctuating experiments were performed using two cut-off ball valves and a cut-off timer (T) to control the inlet gas flow of oxygen and nitrogen gas into the bioreactor (Figure 1). Oxygen is controlled using one ball valve that opens when powered on and closes when powered off. Conversely, the nitrogen is controlled using the other ball valve that closes when powered on and opens on powered off. An infinite cycle timer is used to control both ball valves, and the switching time between nitrogen and oxygen is less than 1 s for the whole device, so that the switching time between the two gases can be ignored. It should be noted that the gas flow entering the vessel remained constant at 2 L/min throughout the whole experiment such that the gas holdup and thus the dilution rate was not changed. In DO oscillation experiment I (last for 100 h), oxygen and nitrogen were alternatively provided for 25 and 125 s, respectively, resulting a DO fluctuation range of 5%−45% within one cycle of 150 s. In DO oscillation experiment II (last for 80 h), oxygen and nitrogen were alternatively provided for 35 and 115 s, respectively, resulting in a DO fluctuation range of 10%−60% within one cycle of 150 s.

To shed light on the metabolic regulation mechanism of *P. chrysogenum* exposed to the above industrial-relevant fluctuating DO conditions, a well-established rapid sampling, quenching and extraction protocol was applied to obtain metabolite dynamics both extracellularly and intracellularly. In both DO oscillation phases, 1.2 mL of each sample for intracellular metabolite quantification was taken every 10 s and a total of 16 samples were obtained in a 150 s complete DO fluctuating cycle. Samples for determination of cell dry weight (CDW), product and by-products were taken every 12 h throughout the cultivation process.

2.5 | CDW

CDW was measured by the weight difference between empty glass fiber filters and dry glass fiber filters (47 mm in diameter, 1 µm pore size, type A/E; Pall Corporation) with biomass. About 15 mL of broth

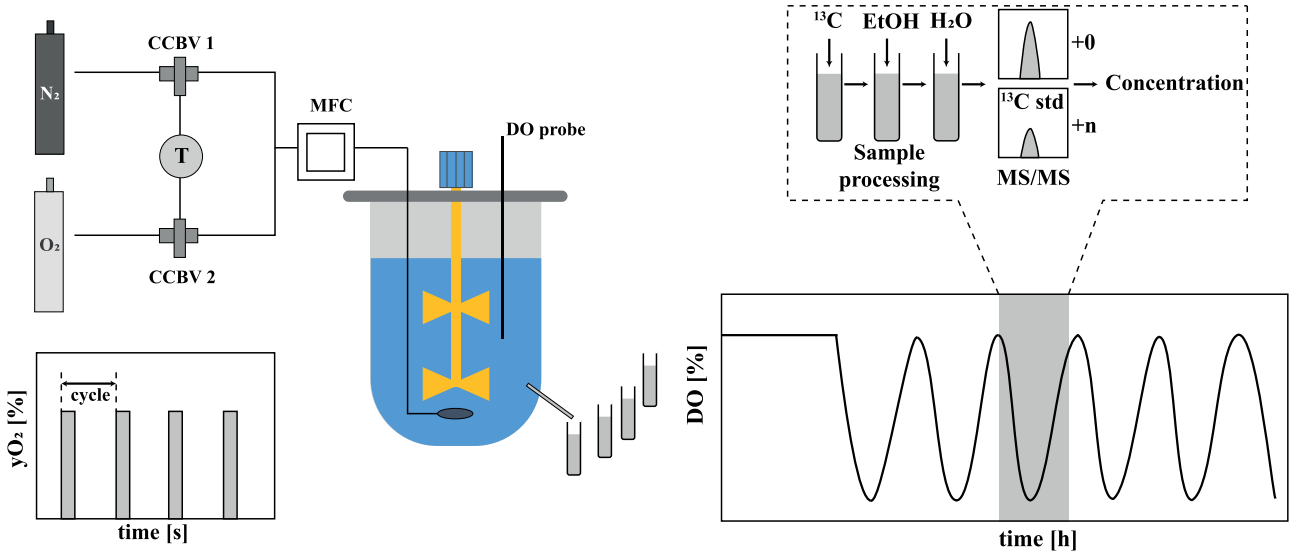

FIGURE 1 Experimental setup for the simulations of fluctuating DO profiles in the glucose-limited chemostat cultures of a high-producing *Penicillium chrysogenum* strain by means of periodically fluctuating oxygen fractions in the inlet gas. In both DO oscillation phases, rapid sampling for measurement of intracellular metabolite was performed during a complete DO fluctuating cycle. DO, dissolved oxygen.

was sampled and split into three portions for CDW measurements (Wang et al., 2019). For each CDW sample, 5 mL of the broth was filtered, and the cell cake was washed three times with 10 mL of demineralized water and dried at a microwave oven (power 800 W) for 4 min. Then, the filter containing biomass was cooled to room temperature in a desiccator and weighed.

2.6 | Rapid sampling, quenching, and metabolite extraction

For extracellular sampling, the cold steel-bead method combined with liquid nitrogen was used for the fast filtration and quenching of extracellular enzyme activities, as described previously (Wang, Wang, et al., 2019). For intracellular sampling, approximately 1.2 mL of broth was taken from the bioreactor into a tube containing the quenching solution (−27.5°C, 40% V/V aqueous methanol). A customized rapid sampling device was developed to ensure fast sampling and rapid quenching, avoiding as much as possible changes in intracellular metabolites. For detailed sampling procedures, please refer to Li et al. (2018). A rapid filtration and cold washing method was used to quickly and efficiently remove all compounds present outside the cells. In this study, a previously established protocol for rapid sampling, quenching, and subsequent metabolite extraction was followed, as previously described (Wang, Chu, et al., 2019). For quantification of intracellular metabolites, isotope dilution mass spectrometry (IDMS) method was used to correct most aspects of analytical bias (Mashego et al., 2005). To achieve this, U-^{13}C-labeled cell extracts obtained from *Pichia pastoris* fed-batch cultures were added as internal standards in the sample before intracellular metabolite extraction (Wu et al., 2005).

2.7 | Analytical methods

Intracellular amino acids (AAs), sugar phosphates, organic acids, and sugar alcohols were quantified by gas chromatography-mass spectrometry (7890 A GC coupled to 5975 C MSD; Agilent Technologies) using the IDMS method, as described previously (Wang, Chu, et al., 2019). The analytical procedures were performed according to (de Jonge et al., 2014) with slight modifications in the column and temperature gradients. For specific settings, please refer to Liu et al. (2019).

An Agilent Zorbax SB-C_{18} reversed-phase column (150 × 4.6 mm ID, 5 µm) was used to determine the concentrations of PAA, penicillin G (PenG), and by-products associated with the penicillin biosynthetic pathway using isocratic gradient reversed-phase high-performance liquid chromatography. The mobile phase was 0.44 g/L KH_2PO_4 in acetonitrile/water (65/35, V/V) and the pH was set between 2.75 and 2.80 using phosphoric acid; the injection volume was 5 µL, the detection wavelength was 214 nm, the flow rate was 1.5 mL/min and the column temperature was 25°C (Wang, Wang et al., 2019).

2.8 | Cytosolic free NADH/NAD$^+$ ratio

The cytosolic free nicotinamide adenine dinucleotide hydrogen/nicotinamide adenine dinucleotide (NADH/NAD$^+$) ratio was estimated using an equilibrium pool of C_4 (aspartate and malate) in the TCA cycle under the assumption of constant K' and intracellular pH (Nasution, van Gulik, Kleijn, et al., 2006; Wang, Wu, et al., 2018):

$$\frac{\text{NADH}}{\text{NAD}^+} = K' \frac{\text{Malate} \times \text{Glutamate}}{\alpha\text{KG} \times \text{Aspartate} \times \text{H}^+} \quad (1)$$

2.9 | Intracellular NADPH/NADP$^+$ ratio

The intracellular NADPH/NADP$^+$ ratio can be calculated based on the reaction catalyzed by glutamate dehydrogenase (GDH), which is supposed to be near equilibrium and assuming constant NH_4^+ concentration and the equilibrium constant (K_{GDH}) of the GDH reaction.

$$\frac{NADPH}{NADP^+} = K_{GDH}\frac{Glutamate}{\alpha KG \times NH_4^+} \quad (2)$$

2.10 | Oxygen uptake rate (OUR) reconstruction

The DO level detected with a commercial optical DO sensor (VisiFerm DO ECS 120 H2, Hamilton, Hamilton Bonaduz AG) were first converted to $C_{O_2,L,FTT}$, by the Fast Fourier transform, to remove the background noise and further corrected by dynamic regression:

$$C_{O_2,L}(\%) = \tau_{r,C_{O_2}} \cdot \frac{dC_{O_2,FTT}}{dt} + C_{O_2,L,FTT} \quad (3)$$

According to the sensor manufacturer, each DO value was calculated based on the average value of previous five measurements in 5 s. So, in this study, the probe delay time ($\tau_{r,C_{O_2}}$) was set at the fixed value of 5 s.

Then, the relative concentration of DO ($C_{O_2,L}$) was converted to its absolute oxygen concentration (C_{O_2}):

$$C_{O_2}\left(\frac{mmol}{L}\right) = C_{O_2,L}\cdot\frac{f_{O_2,air}\cdot p_{fer}}{H_{O_2}} \quad (4)$$

Here, $f_{O_2,air}$ is the fraction of oxygen in the inlet gas, p_{fer} is the pressure of the fermenter, and H_{O_2} is the Henry constant for oxygen at standard condition.

The derivative of the absolute DO concentration with time were obtained by difference method:

$$\frac{d(C_{O_2}|t_n)}{dt} = \frac{C_{O_2}|t_{n+1} - C_{O_2}|t_{n-1}}{t_{n+1} - t_{n-1}} \quad (5)$$

The *P. chrysogenum* cells in the reactor were inactivated at the end of the experiment to keep the OUR value at zero. The periodic DO change was reconstructed with the same oxygen supply strategy to obtain the saturated DO concentration $C^*_{O_2}$:

$$C^*_{O_2} = \frac{d(C_{O_2})}{dt}\cdot\frac{1}{k_L\alpha} + C_{O_2} \quad (6)$$

Finally, the reconstructed OUR value can be calculated according to the following equation:

$$OUR = k_L\alpha\cdot(C^*_{O_2} - C_{O_2}) - \frac{d(C_{O_2})}{dt} \quad (7)$$

2.11 | Model construction

All measured intracellular metabolites and extracellular glucose were utilized to generate the exchange rates. The dynamic profile of these intracellular metabolites was firstly fitted using Splinefit function in MATLAB (R2021b). Then, the derivatives of the fitting curves were calculated and taken as the exchange rates. Finally, 27 metabolite concentration derivative values during each time step window between two samples were calculated. Meanwhile, the reconstructed OUR was used to generate the biomass specific OUR (q_{O_2}) as a function of time. Since one oscillating period is 150 s which is much shorter than the whole fermentation period, the biomass concentration is assumed constant. Also, it is assumed that the biomass composition does not change during the observation time. The time step was taken as 1 s, and the derivative values obtained as well as q rates (q_{O_2} and q_s) were taken as the model inputs. In this work, the *P. chrysogenum* iAL1006 genome-scale metabolic model (GSMM) was obtained from (https://github.com/SysBioChalmers/RAVEN/tree/main/tutorial) (Agren et al., 2013). A new iAL1006D GSMM was generated with 27 dynamic metabolic pools and the original model. More details can be referred from (Liu, Hua, et al., 2021). With the new model, fluxes under steady state were simulated when the lower and upper boundaries for all dynamic reactions were set to zero. Fluxes under a DO fluctuating cycle were simulated when the metabolic concentration derivative values (exchange rates) were utilized as constraints of these dynamic reactions. Normally, the biomass specific growth rate is set as the optimization objective under steady state conditions. However, in this study, we want to compute those constraining fluxes which were dynamic fluxes at each time point. Thus, at each particular time point, the maximization of the biomass growth used as the optimization objective will lead to the same biomass growth rate, rendering it an unsuitable optimization objective. To better investigate the variations in energy metabolism, such as adenosine triphosphate (ATP), throughout the fluctuating DO period, we have shifted our optimization objective to maximizing ATP maintenance. It works as an objective for maximizing ATP production because to consume the maximum amount of ATP, the network must first produce ATP by the most efficient pathways available by recharging the produced ADP. The linear programming solver Gurobi5 (v9.5.1) was used to solve the problem.

3 | RESULTS AND DISCUSSION

3.1 | Generating industrial-relevant DO feast/famine cycles for metabolic studies

In industrial fermentations, each cell experiences the alternating high and low DO concentration at a different frequency and duration of exposure, depending on the circulation loop it follows (de Jonge et al., 2011). To develop a representative DO scale-down setup, we purposely considered three important factors: (i) the duration of the stress, that is, time in which the culture is exposed to low DO environments (below 20% air saturation); (ii) the magnitude of the stress, that is, the strength of DO concentration gradients; and (iii)

the number of times a particular cell goes through a cycle, which is the frequency of exposure to the stress. Towards this goal, based on the registered DO values in the upper and lower layer of 100 and 150 m^3 penicillin production vessels (Goldrick et al., 2015; Haringa et al., 2016), it can be roughly estimated that *P. chrysogenum* cells under this similar production scale can experience DO concentration gradients within the magnitude of 0.05–0.18 mol/m^3.

To estimate the frequency at which cells observe fluctuations, mixing data is required. Measurements of the mixing time in large scale vessels are rare; often, correlations or simulations are used to estimate the mixing time τ_{mix} (Groen, 1994). Jansen et al. (1978) used radiotracers to quantify the mixing time in penicillin production vessels of various scales, as reported in Table 1; for large-scale reactors, a mixing time τ_{mix} of 1–2 min is observed. However, the frequency of environmental fluctuations observed by microbes relates to the circulation time, which as a rule of thumb is estimated as $\tau_{circ} = \frac{\tau_{mix}}{4}$. In any case, for the given industrial-scale mixing times, a circulation and hence fluctuation time in the order of 30–45 s is expected, which is in accordance with the circulation time measured in the 54 m^3 penicillin fermentor considered by Haringa et al. (2016). Practically, the realization of sub-minute fluctuations in bench-scale reactors is problematic, which is why a fluctuation duration of 150 s was chosen in this study.

According to the DO control strategy in this study, the entire cultivation process can be divided into three phases: the first phase (0–120 h), the DO level was maintained at 60% (0.18 mol/m^3) air saturation; the second phase (120–220 h), a 150 s DO feast/famine cycle fluctuated from 5% (0.015 mol/m^3) to 45% (0.135 mol/m^3) air saturation was reproduced; the third phase (220–300 h), a 150 s DO oscillating cycle fluctuated from 10% (0.03 mol/m^3) to 60% (0.18 mol/m^3) air saturation was reproduced. As shown in Figure 2, we obtained reproducible patterns as indicated by DO dynamics and the derived OUR profiles. In addition, triplicate measurements of both intra- and extracellular metabolite concentration during three individual experiments were taken to check the reproducibility of the cycles. Taken together, these measurements suggest a high reproducibility of the cycles and the sampling protocol (Figures 3–4).

TABLE 1 Mixing times in different sizes of penicillin production vessels for H/T = 2.5.

V_L (m^3)	T (m)	P (kW)	P/V (kW/m^3)	t_m (s)
1.4	1.1	3.8	2.7	29
45.0	3.5	120.0	2.7	67
190.0	4.4	240.0	1.3	119

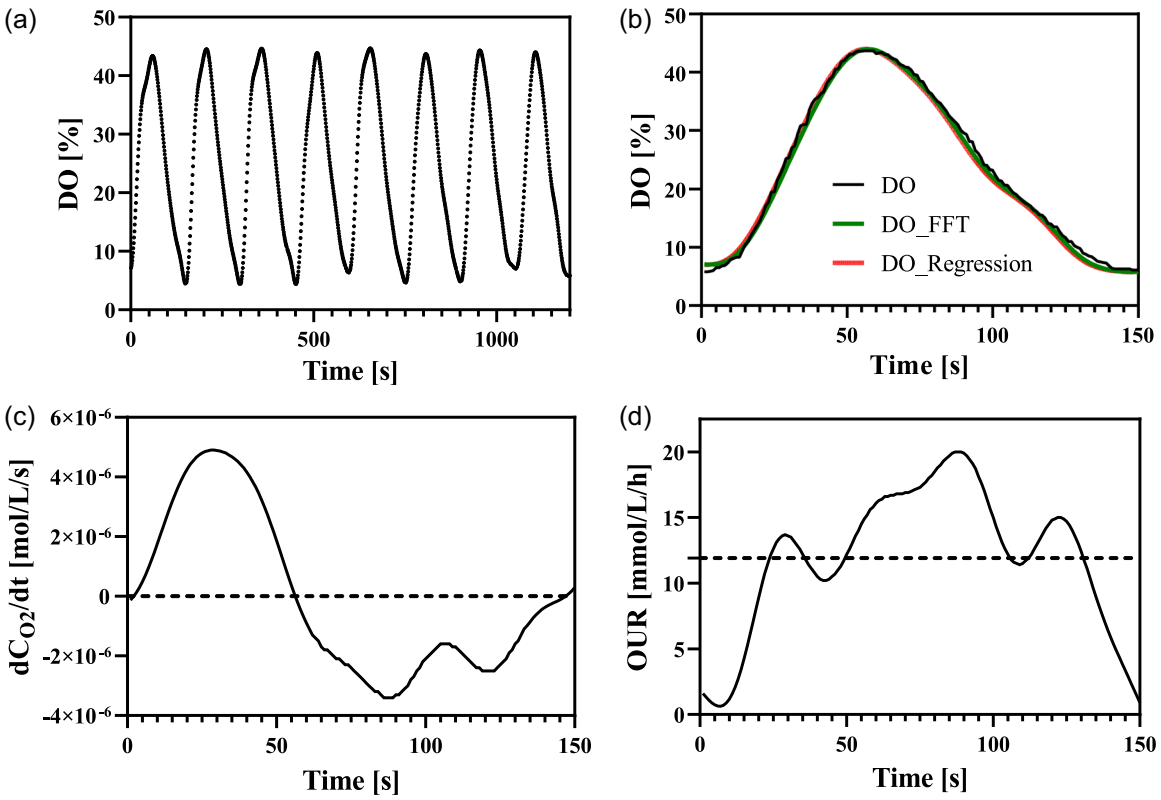

FIGURE 2 Reconstructed OUR in the periodic dissolved oxygen (DO) fluctuation experiment. (a) Periodic variation of DO over 8 cycles and (b) one cycle in the periodic DO fluctuation experiment. Black line: original DO concentration, green line: DO concentration after fast Fourier transform (FFT) smoothing, and red line: the smoothing DO concentration after dynamic regression calculation. (c) The derivative of the oxygen concentration in one cycle. (d) Reconstructed OUR, dashed line: averaged OUR. OUR, oxygen uptake rate.

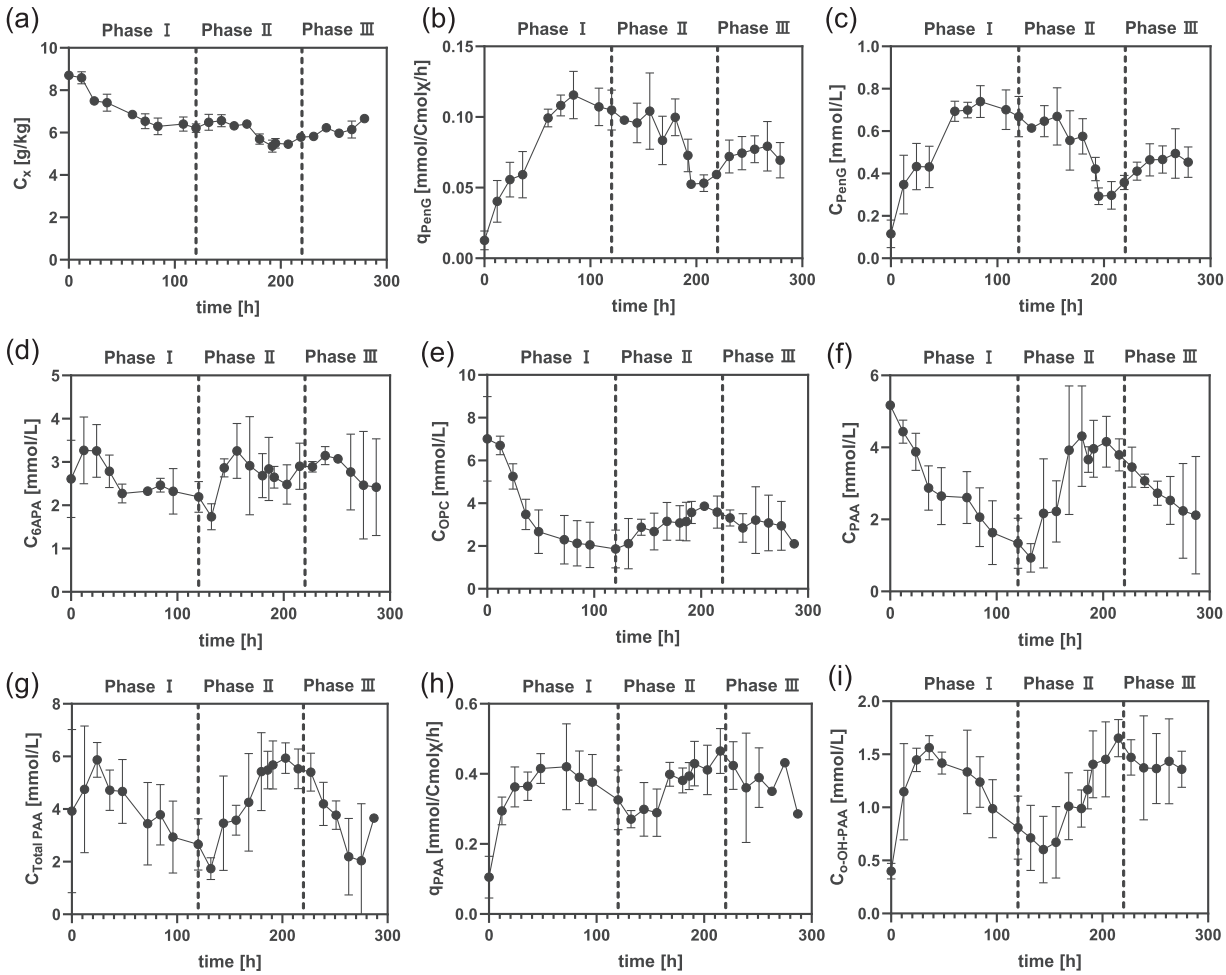

FIGURE 3 Measured concentrations of (a) biomass, (b) the biomass specific penicillin production rate (q_{PenG}), (c) penicillin G (PenG), (d) 6-aminopenicillanic acid (6APA), (e) 6-oxopiperidine-2-carboxylic acid (OPC), (f) phenylacetic acid (PAA), (g) total PAA(C_{PAA} + C_{PenG} + $C_{o-OH-PAA}$), (h) the biomass specific PAA accumulation rate (q_{PAA}), (i) ortho-hydroxyphenyl acetic acid (o-OH-PAA) concentration at DO-oscillation experiments. Phase I (0–120 h): DO steady state condition; Phase II (120–220 h): DO oscillation between 5%–45% within the cycle of 150 s; Phase III (220–300 h): DO oscillation between 10%–60% within the cycle of 150 s. Error bar represents the error of three biological replicates. Time 0 signifies the start of chemostat cultivation.

3.2 | Prolonged periodic DO fluctuation responsible for performance loss

Figure 3 shows the dynamic profiles of extracellular product, by-product and the biomass specific rates. As shown in Figure 3a, CDW showed a first decrease and then basically stabilized at about 7 g/kg during the first phase, which has been often observed during the switch from batch to chemostat cultivation. In the second phase, after being exposed to DO fluctuating cycles from 5% (0.015 mol/m^3) to 45% (0.135 mol/m^3) air saturation, the CDW gradually decreased and basically stabilized at about 5 g/kg at the end of the second phase. In this phase, the DO fell below 20% for 50 s during each cycle. In the third phase, DO fluctuating cycles were oscillated in the range from 10% (0.03 mol/m^3) to 60% (0.18 mol/m^3) air saturation and *P. chrysogenum* cell exposure to less than 20% air saturation was decreased to 20 s. As a result, it can be observed that the CDW were gradually increased to about 6 g/kg. This result apparently indicated that the exposure time to the low DO level (less than 20%) imposed a significant impact on the biomass growth. This seems reasonable because our previous study has demonstrated the critical DO concentrations for biomass growth and penicillin production were 5% and 20%, respectively (Yang et al., 2022). However, a recent study by Janoska et al. (2022) observed an opposite trend that the biomass concentration under chemostat cultures was slightly increased in response to oscillating DO conditions with a fluctuation period of 120 s and fluctuation amplitudes of 0–0.127 mol/m^3 and 0–0.178 mol/m^3. This observed difference may be ascribed to different fluctuation amplitudes and different strains applied in this study. Additionally, it should be noted that in all DO-perturbation regimes, the fungus grew as dispersed mycelia and no significant morphological differences were observed under the microscope.

In addition, DO fluctuations also have a considerable effect on the biosynthesis of penicillin and by-products. As shown in Figure 3b, the biomass specific PenG production rate (q_{PenG}) showed a first

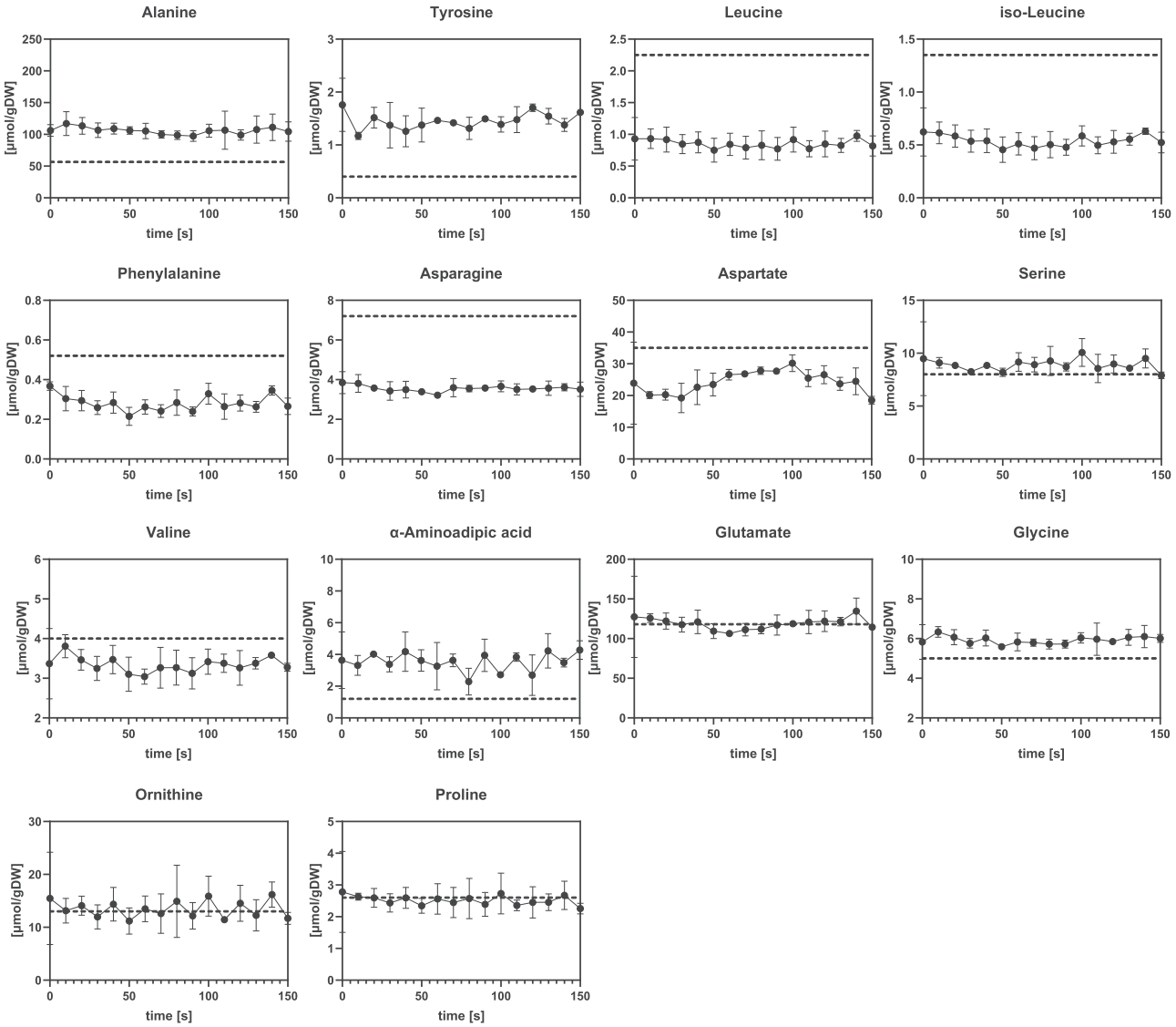

FIGURE 4 Intracellular amounts of amino acids (AAs) in *Penicillium chrysogenum* Wisconsin 54−1255 under DO-oscillation experiments. The DO concentration fluctuates between 5% and 45% within 150 s. Time 0 represents the beginning of DO feast/famine cycle. The dash line represents the average AA amounts in the control group. Error bar represents the error of three biological replicates. DO, dissolved oxygen.

increase and then basically stabilized at 0.091 mmol/CmolX/h in the first phase, which is consistent with our previous results (0.096 mmol/CmolX/h) at 60% DO steady state experiments (Yang et al., 2022). After the start of periodic DO fluctuations in the Phase II, the penicillin concentration and the q_{PenG} gradually decreased, and the q_{PenG} after 100 h of DO oscillation between 5% and 45% in the cycle of 150 s was considerably reduced by a factor of two compared to that of 60% steady-state DO conditions. To reduce the exposure time to DO below 20%, DO was oscillated between 10% and 60% in the cycle of 150 s in the Phase III. As anticipated, the results showed that penicillin concentration was gradually increased (Figure 3c) and the q_{PenG} was considerably recovered by 28.6% relative to that at the end of the Phase II (Figure 3b). Furthermore, our previous study has demonstrated that in comparison with the reference control (60% DO), the penicillin productivity was reduced by 25% at a DO value of 5% under steady state conditions. Only a 14% reduction in penicillin productivity was observed as the DO level was ramped down to 0% (Q. Yang et al., 2022). Combining this with the results in the present study, we can arrive at the conclusion that periodic DO fluctuations around the critical value have a much more pronounced effect on the penicillin production capacity in the *P. chrysogenum* Wisconsin 54−1255. This is consistent with the results of Janoska et al. (2022). Their study also demonstrated that oscillations of DO level ranging in 0−0.127 mol/m^3 and 0−0.178 mol/m^3 with the cycle time of 120 s both can result in a more severe decrease in penicillin productivity compared to the one-step decrease in DO level from 0.139 to 0.190 mol/m^3 to 0.025, 0.013, and 0.009 mol/m^3. Taken together, as typically occurring in the industrial-scale bioreactor, periodic exposure to high/low DO leads to more severe production performance loss as compared to short-term or long-term low DO

exposure. This seems reasonable because cells sense and respond to these dynamic DO perturbations leading to frequent activation of their regulatory programs, which are mostly achieved at the expense of extra ATP for cellular maintenance (Loffler et al., 2016; Simen et al., 2017).

As shown in Figure 3d-i, the precursor PAA and other byproducts (i.e., 6APA, OPC and ortho-hydroxyphenyl acetic acid [o-OH-PAA]) associated with penicillin biosynthetic pathway are measured throughout the cultivation process. It is apparent that after 100 h DO oscillation in Phase II the major byproducts 6APA and OPC were significantly accumulated by 33% and 47%, respectively, as compared to those at the end of the first phase (Figure 3d,e). Interestingly, when the cells were exposed to higher DO variations and no periods of below 10% DO, three major by-products showed a decreasing trend over the time. This seems reasonable because the penicillin production capacity was partly recovered in the third phase and thus more carbon in the penicillin biosynthetic pathway was directed towards penicillin production rather than byproduct accumulation. Meanwhile, PAA is the essential precursor for the production of PenG. To ensure that PAA is neither limiting for product formation nor toxic for biomass growth, PAA in the feed was set at a concentration of 5 mM (Wang et al., 2019). Similarly, due to the variation in the penicillin production capacity, the extracellular PAA concentration shows an increasing and decreasing trend, respectively, in Phase II and Phase III (Figure 3f). In *P. chrysogenum* Wisconsin 54−155, PAA can be either assimilated into penicillin or hydroxylated to form the by-product o-OH-PAA, which can be further metabolized as the auxiliary carbon source (Eriksen et al., 1998). It can be seen in Phase I that only 20% of the supplied PAA was incorporated into benzylpenicillin while the rest was metabolized (Figure 3c,f) and cumulative concentration of extracellular PAA, PenG and o-OH-PAA shows a decreasing trend and deviates from the total PAA concentration of 5 mM in the feed, which indicates a gradual induction of PAA catabolism (Figure 3g). Although the penicillin production capacity was substantially decreased after the initiation of DO fluctuation, the biomass specific PAA consumption rate was significantly increased in Phase II (Figure 3h). Interestingly, the PAA recovery was becoming closer to 100% at the end of Phase II (Figure 3g), which suggests that PAA was metabolized slower than before as the carbon source during the DO fluctuating cycles. Also, the extracellular PAA was accumulated rather than converted into the by-product o-OH-PAA. This can be explained by the fact that o-OH-PAA is formed from PAA by hydroxylation and the PAA hydroxylase (PAH) responsible for the conversion requires oxygen (Rodriguez-Saiz et al., 2001).

Additionally, when *P. chrysogenum* cells were exposed to higher DO variations and no periods of below 10% DO in Phase III, the extracellular o-OH-PAA and PAA were decreased together with the gradual increase of penicillin productivity (Figure 3f,i). Meanwhile, the PAA recovery was gradually deviating from 100% in this phase. This phenomenon suggests that the cellular exposure time to low DO may repress the enzymatic activity of PAH responsible for PAA hydroxylation. However, our recent study has demonstrated that during the DO steady state cultures (60%, 20%, 10%, and 5%), the total recovered PAA first decreased and then largely stabilized at 2 mM throughout the cultivation process. Also, in the DO ramp-down experiments, a similar trend in the extracellular PAA concentration was observed before DO ramp-down, and total recovered PAA gradually increased from 2 to 3 mM after a linear decrease of DO from 60% to 0 within 24 h. Taken together, the results of the present study suggest that from an economic point of view, it is interesting to note that in highly dynamic DO environments not only the penicillin productivity was reduced, but also that of the byproduct o-OH-PAA, which cannot be recycled. Probably, the DO fluctuation leads to lower expression levels and/or activities of PAA 2-hydroxylase, which should be further verified in the following study.

3.3 | Adaptation of central metabolite pools to oscillating DO conditions

3.3.1 | Intracellular AAs

Intracellular AAs are key precursors for cell growth and penicillin biosynthesis, and hence it is of great importance to investigate the time patterns of intracellular AA pools under DO oscillating conditions. There were a few AAs whose intracellular pool size decreased or increased with the fluctuation of DO (Figure 4). For example, intracellular pool size of alanine and tyrosine was much higher than that of the control group, while intracellular pool size of leucine, isoleucine, phenylalanine and asparagine was much lower than that of the control group. Among them, tyrosine and asparagine showed the most pronounced increase and decrease in intracellular pool size, respectively, in response to oscillating DO cycle. During the 150 s cycle of oscillating DO, the DO concentration went up from low (5%) to high (45%) and then to low (5%). Contrast to this oscillating DO dynamics, AAs such as serine, aspartate, leucine, isoleucine and phenylalanine showed a trend of decreasing and then increasing during the cycle, indicating there may be an inverse correlation with the DO dynamics. However, the results showed that eight of 14 intracellular AA pools measured did not change significantly from the control amounts at steady state at a DO of 60% during one complete oscillating DO cycle, including aspartate, serine, valine, α-aminoadipic acid, glutamate, glycine, ornithine and proline (Figure 4).

In our previous scale-down study of substrate gradients by means of a 6-min on−off feeding regime, we also have observed that intracellular pool size of leucine and isoleucine were first decreased followed by an increase during the cycle (Wang, Chu, et al., 2019). After comparing the substrate gradient results with those during the fluctuating DO condition, it was found that intracellular leucine and isoleucine were mobilized at approximately the same magnitude, with leucine and isoleucine fluctuating between 0.8 and 1.2 μmol/gDW and 0.4−0.7 μmol/gDW, respectively. Meanwhile, in contrast with the intracellular aspartate pool dynamics under the oscillating DO condition, the opposite trend was observed under substrate feast/

famine cycles, but the fluctuating range of intracellular pool size was also basically the same (20–30 μmol/gDW). In addition, intracellular amounts of serine and asparagine were essentially the same and stable during cyclic fluctuations of both DO and substrate, while the average intracellular amounts of alanine and glutamate during the fluctuating DO condition was twice as high as those under the fluctuating substrate condition. Overall, the variation in the intracellular AA pools size was much more pronounced in terms of both coverage and magnitude under repetitive substrate pulses than under DO fluctuations (Wang, Chu, et al., 2019). In addition, the three precursor AAs, that is, cysteine, valine and α-aminoadipic acid, are essential for the production of penicillin. Intracellular α-aminoadipic acid amount was about two times higher, while intracellular valine showed a little bit lower in the DO oscillating condition than in the control (Figure 4). However, since the δ-(L-α-aminoadipic acid)-L-cysteine-D-valine synthase (ACVS) has lower affinity coefficients (45, 80, and 80 μM) for all three precursor AAs, the decrease in precursor concentration may not be the main reason for the decreased penicillin production capacity (Theilgaard et al., 1997). Rather, the reduced penicillin productivity may lead to a lower cellular demand for these precursor AAs.

3.3.2 | Intracellular sugar phosphates, organic acids, and sugar polyols

The oscillating DO may also influence substrate uptake kinetics of *P. chrysogenum*. It can be seen from Figure 5 that the intracellular glucose level under oscillating DO condition (2.7 mM) is significantly lower than under 60% DO steady state condition (7 mM), while it is

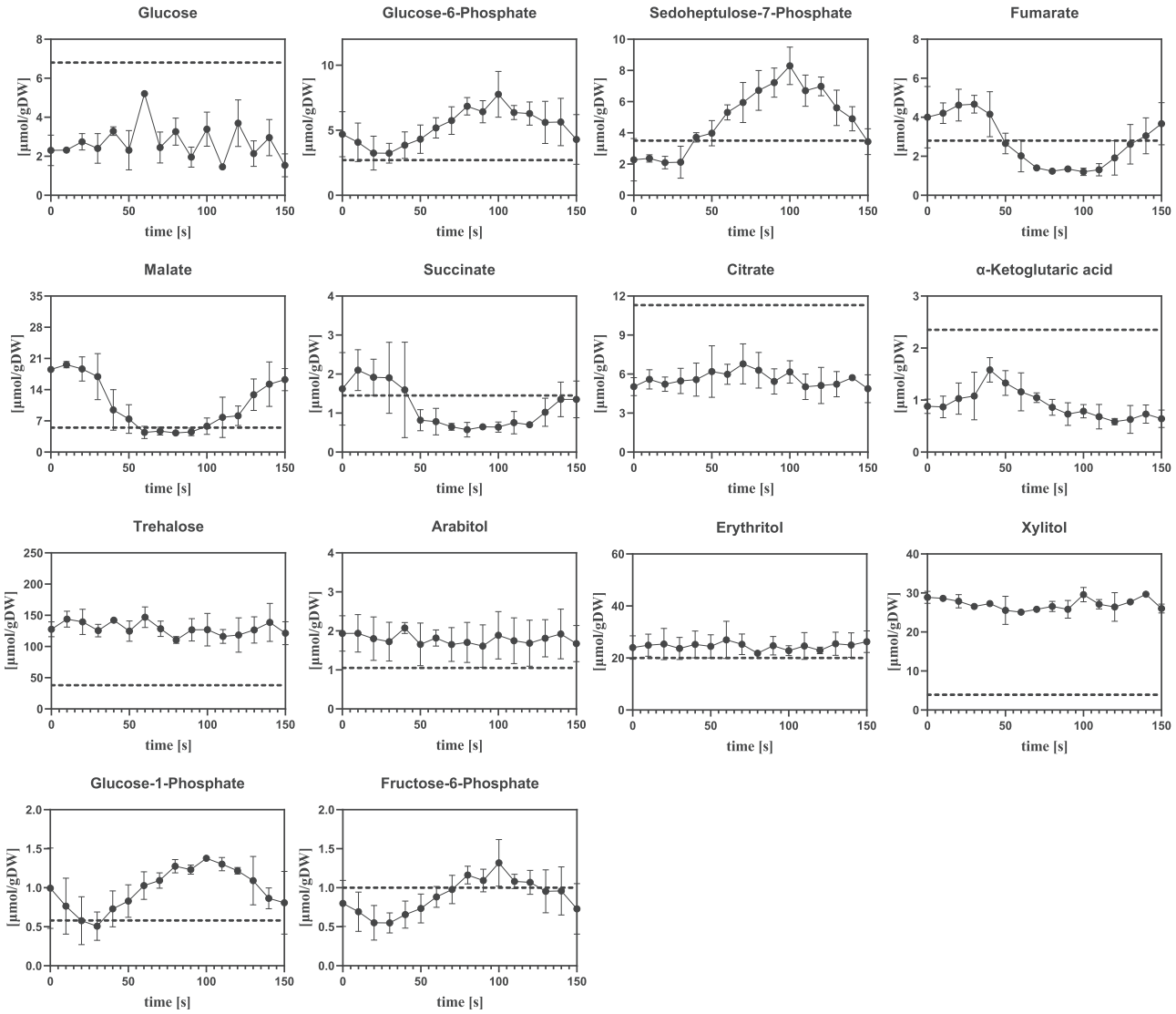

FIGURE 5 Intracellular amounts of sugar phosphates, organic acids, and sugar polyols in *Penicillium chrysogenum* Wisconsin 54–1255 under DO-oscillation experiments. The DO concentration fluctuates between 5% and 45% within 150 s. Time 0 represents the beginning of DO feast/famine cycle. The dash line represents the average intracelluar amounts of measured metabolites in the control group. Error bar represents the error of three biological replicates. DO, dissolved oxygen.

basically consistent with the intracellular glucose level when DO was ramped down to 5% (3.1 mM). This shows that the intracellular glucose concentration is inclined to be lower when the cells are under both oxygen limitation and oscillation conditions. For example, in the yeast *Saccharomyces cerevisiae*, it has been reported that a high intracellular glucose concentration can reduce the glucose transport rate by 50% (Teusink et al., 1998). Thus, keeping a low intracellular glucose concentration is somewhat instrumental in facilitating glucose uptake under unfavorable oxygen availability. In this study, the average biomass specific glucose consumption rate (q_s) during DO fluctuations was 18.18 mmol/CmolX/h, which was not significantly different ($p > 0.05$) from that at 60% DO steady state (18.06 mmol/CmolX/h) conditions. This implies that the oscillating DO strategy adopted in this study does not significantly influence the glucose uptake kinetics in *P. chrysogenum* under glucose-limited conditions.

As similarly observed in previous scale-down study of substrate gradients for *P. chrysogenum* (Wang, Chu, et al., 2019), it is apparent that intracellular sugar phosphates and organic acids show dynamic patterns exposed to the fluctuating DO condition (Figure 5). The results showed that average intracellular organic acid and sugar phosphate amounts were essentially the same after undergoing the fluctuating DO condition. During the DO oscillating cycle, the dynamics of intracellular glucose-6-phosphate (G6P) and sedoheptulose 7-phosphate (S7P) was synchronized with the oscillating DO, showing a decreasing trend at low DO and a rapid increase when the DO increased. An interesting phenomenon is the uncoupling behavior of intracellular glucose to its downstream metabolite G6P. This seems reasonable that the conversion from glucose to G6P catalyzed by hexokinase involves the consumption of ATP. When there is an energy deficit and imbalanced redox state under the low DO condition, it definitely affects the production of G6P. Additionally, cells that constrained by ATP supply are predisposed to rearrange pathways that require less energy. For example, the carbon flux may be more directed toward PP pathway to keep balanced metabolic state. When the DO becomes abundant, the accumulation of G6P can be recovered. Compared to substrate oscillation (Wang, Chu, et al., 2019), DO oscillation gave rise to a lower average pool size of sugar phosphates in both Embden-Meyerhof-Parnas (EMP) pathway and pentose phosphate (PP) pathway. Contrary to the DO dynamics, intracellular fumaric acid, succinic acid and malic acid in the TCA cycle showed a dynamic trend of decreasing and then increasing during the cycle. Meanwhile, in concert with the changing DO, intracellular amounts of citric acid and α-ketoglutaric acid showed a rising and then decreasing trend. This may be ascribed to the relatively small pool size of these metabolites and the susceptibility of the levels to fluctuating environments. As compared to substrate oscillations (Wang, Chu, et al., 2019), the oscillating DO led to more pronounced dynamics of intracellular organic acids. However, the average organic acid amounts were basically the same under both oscillation conditions. Moreover, the cytoplasmic reduction state also affects the levels of these metabolites. Previous studies have revealed that when the reduction state becomes high under oxygen-limited conditions, the flux of the PP pathway decreases and the flux of the glyoxylate pathway increases, accompanied by the increased intracellular amount of succinate, malate and fumarate (Lu et al., 2018; Yang et al., 2022). The glyoxylate shunt divides the TCA cycle into upper and lower parts, with α-ketoglutarate in the lower part and malate, succinate and fumarate in the upper part. Such opposite changes in the levels of these organic acids also suggest that fluctuations in DO in this study may lead to the suppression of the TCA cycle and the activation of the glyoxylate shunt. This is consistent with our previous results of DO steady state and DO ramp-down experiments, where DO concentrations below 20% resulted in the accumulation of fumarate, malate, and succinic acid. In addition, flux balance analysis also demonstrated that the hypoxic environment may lead to activation of the glyoxylate shunt in *P. chrysogenum* (Yang et al., 2022).

In *P. chrysogenum*, a high content of intracellular carbohydrates, especially reduced sugars such as mannitol, arabitol, erythritol, as well as trehalose and glycogen has been identified, which has been reported to respond adequately to changing environments or perturbations (Zhao et al., 2012). As shown in Figure 5, intracellular sugar polyols including trehalose, arabitol, erythritol and xylitol does not show obvious trends during the oscillating DO cycle mainly because they have a relatively larger pool size and longer turnover times. However, they were significantly higher under dynamic DO conditions compared to the reference DO steady-state conditions. Consistent with this, our previous DO shift-down and DO ramp-down experiments have also shown that intracellular amounts of these sugar polyols were significantly increased with decreasing DO concentration (Yang et al., 2022). More interestingly, intracellular trehalose and xylitol levels were threefold and twofold higher under the DO oscillation condition than those under 5% DO steady state condition, while they became 10-fold and fourfold higher than those under 0% DO ramp-down condition, respectively. Several previous studies have reported that adverse cultivation environments can induce the accumulation of sugar polyols to fulfill their physiological roles for example, act as carbohydrate reserves, reducing power reservoir in *P. chrysogenum* (de Jonge et al., 2014; Wang, Zhao, et al., 2018; Zhao et al., 2012). For example, in *Aspergillus niger* polyols were the main metabolic products formed and represented up to 22% of the carbon consumed in oxygen-limited conditions (Diano et al., 2006). Thus, polyols become hallmark metabolites for the cells to cope with the adverse environment. In this study, DO was fluctuated around the critical values for cellular respiration and penicillin production by *P. chrysogenum*, which most probably induced the cell to reserve these sugar polyols as both carbon source and the reservoir of reducing equivalents. Taken together, periodic exposure to high/low DO leads to more pronounced accumulation of sugar polyols as compared to short-term or long-term low DO exposure.

3.3.3 | Dynamic patterns of intracellular metabolite groups

Figure 6 shows the dynamic profiles of the amount of carbon in groups of intracellular metabolites, such as groups of AAs, central

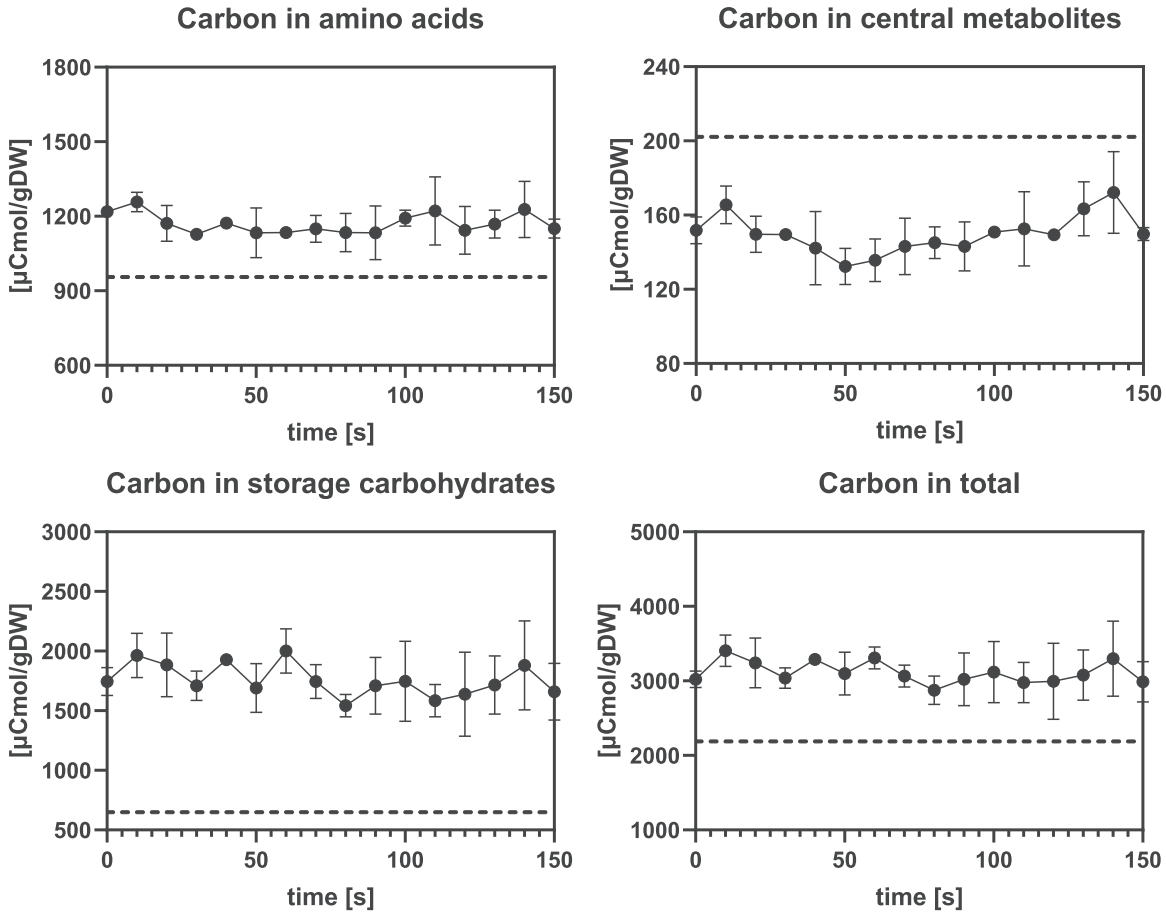

FIGURE 6 Intracellular carbon pool under DO-oscillation experiments within a complete DO oscillating cycle. The DO concentration fluctuates between 5% and 45% within 150 s. Time 0 represents the beginning of DO feast/famine cycle. The dashed lines represent the average intracelluar amounts of carbon pools in the control group. Error bar represents the error of three biological replicates. DO, dissolved oxygen.

metabolites and storage carbohydrates under both 60% DO steady state and oscillating DO experiments. Interestingly, it was observed that under DO oscillating condition, intracellular pool sizes of AAs and storage carbohydrates were significantly higher while central metabolites were lower as compared to those under 60% DO steady state condition. The lower pool size of central metabolites can in principle lead to decreased turnover time which facilitates fast adaptation of cellular metabolism to dynamic environmental perturbation.

Despite the opposite trends, the intracellular pool size of the central metabolite displayed strong dynamics in concert with the oscillating DO (Wang, Chu, et al., 2019). Additionally, it is reasonable that more carbon from the glucose will be directed to intracellular AAs and storage carbohydrates since there is no significant difference of the q_s under the DO oscillating condition as compared to that under 60% DO steady state conditions. Previous studies have demonstrated that an increase of storage carbohydrates can adequately buffer the extracellular dynamics in substrate supply (de Jonge et al., 2014; Wang, Zhao, et al., 2018). In this study, DO oscillation around the critical values for cellular respiration most likely hampered the regeneration of NAD^+ and thus the elevated NADH/NAD^+ ratio can make the glycolytic flux less thermodynamically favorable (Canelas et al., 2008). For example, it has been shown that glucose consumption rate critically depends on the cellular redox state, which was indicated as the NADH/NAD^+ ratio, in *Corynebacterium glutamicum* under oxygen deprivation (Tsuge et al., 2015). However, the q_s value under the DO oscillation did not significantly change, which implies there might be redox stress-alleviating strategies and/or the glucose uptake system in *P. chrysogenum* seems insensitive to the perturbation of the cytosolic NADH/NAD^+ ratio.

3.3.4 | Cytosolic NADH/NAD^+ and NADPH/$NADP^+$ ratios

To investigate the intracellular redox potential upon such DO oscillating condition, the C_4 equilibrium pool (aspartate and malate) in the TCA cycle was used to indirectly estimate the cytoplasmic redox status in terms of NADH/NAD^+ ratio (Nasution, van Gulik, Proell, et al., 2006; Wang, Wu, et al., 2018). As shown in Figure 7, the free cytosolic NADH/NAD^+ ratio tended to decrease followed by an

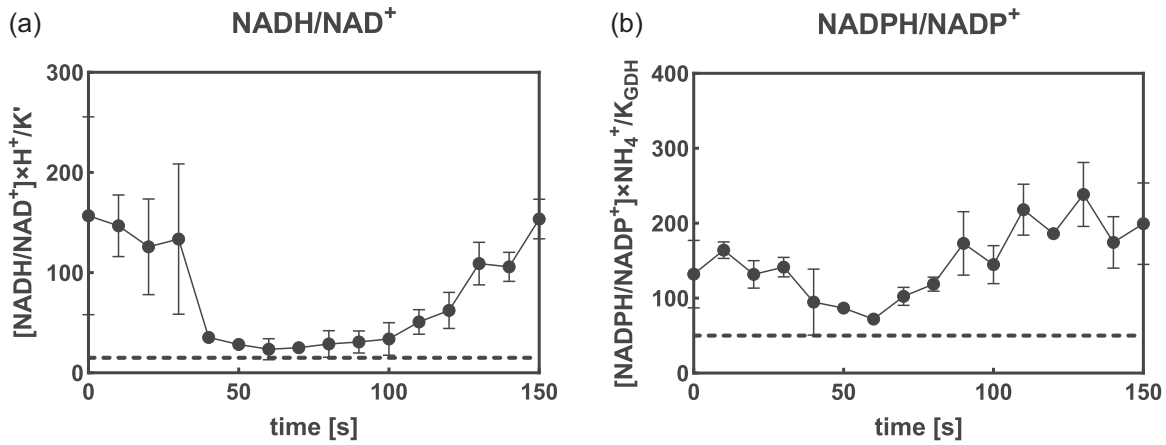

FIGURE 7 Calculated NADH/NAD$^+$ and NADPH/NADP$^+$ ratios over the DO oscillation cycle. The DO concentration fluctuates between 5% and 45% within 150 s. Time 0 represents the beginning of DO feast/famine cycle. The dashed lines represent the average values of the cytosolic NADH/NAD$^+$ and NADPH/NADP$^+$ ratios in the control group. Error bar represents the error of three biological replicates. DO, dissolved oxygen.

increase over a 150 s cycle, which was opposite to the trend of DO concentration (Figure 2). As previously hypothesized, the intracellular amounts of organic acids, that is, fumarate, malate, and succinic acids, in the TCA cycle are regulated by the cytosolic redox state, which is indeed manifested by the same dynamics over the oscillating DO cycle (Figure 5).

Our previous study has shown that the cytosolic redox state was gradually increased with time during the DO ramp-down experiments, which was accompanied by the gradual decrease of penicillin productivity (Yang et al., 2022). This seems reasonable because a more reduced cytosol may lead to more reduction of sulfur–sulfur bonds in proteins, which disturbs protein folding and therewith activity and/or binding property, regulating gene expression (Giles et al., 2003). Previous studies have already verified that impaired and/or imbalanced expression of the core enzymes in the penicillin biosynthetic pathway might lead to rapid loss of high penicillin production capacity (Deshmukh et al., 2015; Douma et al., 2011; Weber et al., 2012). Hence, this relation should be further verified on the transcript and protein levels; however, this is not within the scope of this study. Consistent with this, the mean cytoplasmic redox state during DO fluctuations was significantly higher than in the 60% DO steady state experiment (Figure 7a), which might further accelerate the deterioration of high penicillin production capacity (Wang, Wu, et al., 2018).

Additionally, previous studies have concluded that in penicillin fermentation, possible limitations in primary metabolism reside in the supply/regeneration of cofactors (NADPH) rather than in the supply of carbon precursors (Kleijn et al., 2007; Thykaer et al., 2008; van Gulik et al., 2000). Here, a metabolite sensor based on the assumed fast equilibrium reaction catalyzed by GDH was used to estimate the cytosolic NADPH/NADP$^+$ ratio in *P. chrysogenum*. As shown in Figure 7b, the cytosolic NADPH/NADP$^+$ ratio shows a sharp decrease followed by a rapid increase trend during the 150 s periodic DO cycle. However, this ratio on the average was significantly higher during DO fluctuations than in the 60% DO steady state experiment, which suggests that the NADPH supply might not be the limiting factor for the penicillin production. The reason for the reduced penicillin productivity could be that the positive NADPH effect may be counteracted by the decreased ATP supply since ATP is also required from primary metabolism for high penicillin production (73 mol of ATP per mole of penicillin-G) (van Gulik et al., 2001). It seems reasonable that ATP and energy charge become the limiting factors when the DO was oscillated around the critical values for biomass growth and penicillin production (Yang et al., 2022).

3.3.5 | Extracellular sugar phosphates, organic acids, and sugar polyols

Supporting Information S1: Figure 1 shows the dynamics of extracellular concentrations of sugar phosphates, organic acids and sugar polyols in response to periodic fluctuations in DO. The results showed that none of these measured extracellular metabolites showed an obvious trend during the 150 s cycle, but their mean concentrations (except for arabitol and succinic acid) were significantly higher than those of the control group. This implies that DO oscillation induces more excretion of intracellular metabolites. It seems reasonable because these metabolites, which are present in large amounts intracellularly (Figure 5), are inclined to accumulate in large quantities extracellularly. Strikingly, our previous study has shown that extracellular glucose concentration increased approximately threefold (14 μM) at 5% DO steady state and increased 25-fold (100 μM) when DO was ramped down to 5% compared to 60% DO steady state (4 μM) conditions (Yang et al., 2022). In this study, the extracellular glucose concentration (50 μM) increased 10-fold compared to the 60% DO steady state condition. This increase can be mostly ascribed to the decrease of biomass concentration under the DO oscillating condition because no significant change in the biomass specific glucose uptake rate

was observed after the start of the oscillation. This increase in extracellular glucose concentration can cause glucose suppression on the supply of precursor AA, for example, aminoadipic acid as well as on the transcription of penicillin gene clusters (Revilla et al., 1986). Hence, the elevated extracellular glucose concentration may partly account for the decreased penicillin productivity under the DO oscillating condition. In addition, different from strong dynamics of extracellular glucose concentration triggered by repetitive glucose pulses (Wang, Chu, et al., 2019), the extracellular glucose concentration remained largely stable at higher concentrations during periodic fluctuations in DO (Supporting Information S1: Figure 1). This differential substrate uptake dynamics may lead to much more pronounced variation in the pool size of intracellular metabolites between repetitive substrate and DO oscillations as described in the previous section.

The above extracellular glucose concentrations also imply that prolonged low DO perturbation may induce a progressive decrease of affinity for glucose, which is most probably accompanied by the elevated expression of low-affinity glucose transporters. However, previous studies have revealed that prolonged exposure to substrate-limited conditions can induce the expression of high-affinity glucose transporter and thus lead to a progressive decrease of the residual glucose concentration (Jansen et al., 2004, 2005). In high-yielding *P. chrysogenum* strain, the evolution of the glucose uptake system with a higher-affinity for glucose will aggravate the formation of more extreme substrate gradients, which has been reported to accelerate strain degeneration and negatively affect the penicillin productivity (de Jonge et al., 2011; Wang, Zhao, et al., 2018). Hence, it is interesting to note that in the large-scale bioreactor, *P. chrysogenum* mostly experiences both gradients of substrate and DO. Under this circumstance not only the formation rate of penicillin will be reduced, but also that of degeneration of penicillin production induced by low glucose sensing (Douma et al., 2011; Wang, Wu, et al., 2018).

3.4 | Adaptation of intracellular metabolic flux to oscillating DO conditions

To further quantitatively explore cellular metabolic adaptation to these oscillating DO conditions, dynamic metabolic flux information as complementary to metabolite concentrations is equally important for metabolic understanding (Jang et al., 2018). To our knowledge, previous studies has mainly focused on the flux distribution analysis under glucose feast/famine conditions with *P. chrysogenum* strains (de Jonge et al., 2014; Zhao et al., 2012). However, little has been known regarding the dynamic flux response upon DO perturbations. Towards this end, in this study, we estimated dynamic metabolic flux by incorporating time-resolved intracellular metabolite measurements into the previously established genome-scale metabolic model for *P. chrysogenum* Wisconsin 54−1255 strain (Agren et al., 2013; Liu, Hua, et al., 2021).

3.4.1 | Evaluation of changing rates of measured intracellular metabolites

In this study, the DO fluctuation was set as shown in the DO oscillation experiment I (See Section 2.4). The DO fluctuation range was maintained between 5% and 45% during a cycle of 150 s. The q_{O_2} profiles were obtained through the OUR reconstruction as described in Section 2.10. The dummy intracellular metabolite concentrations were obtained by a rapid sampling method as described in Section 2.6. The derivative (concentration-time curve) of each measured intracellular metabolite was obtained using Splinefit (as described in Section 2.11). The derivative of metabolite concentration with time represents the accumulation rate of the corresponding metabolite, with positive values indicating accumulation and negative values indicating consumption. These derivative values can be interpreted as virtual changing rates of the corresponding metabolites. For each changing rate, the related dummy reaction could be added to the GEM model. Supporting Information S1: Figure 2 shows the virtual changing rates of central carbon metabolic pathways and AAs metabolic pathways obtained from dummy metabolite concentrations. These virtual changing rates can be used as inputs for calculating intracellular fluxes at each time point using the GEM model.

As shown from Supporting Information S1: Figure 2a, it is apparent that some intracellular metabolites display a rapid and significant response to the increase of extracellular oxygen concentration, especially those measured metabolites in the TCA cycle. The rates of the major metabolites in the TCA cycle exhibited a variation pattern of positive-negative-positive, indicating the changing pattern of related metabolite concentrations. For example, the rates of malate, fumarate, and succinate became negative at approximately 25 s and returned to positive values around 75 s. This suggested that when the concentration of a metabolite accumulates beyond a particular threshold, its production rate decreases or its consumption rate increases. Conversely, the changing rates of metabolites in the PP pathway, such as G6P and S7P, exhibited a negative-positive-negative pattern. The above-mentioned results of changing rates confirmed the different regulation pattern of central carbon metabolism under the DO feast/famine cycle. In contrast, changes in the AA pools are relatively subtle (Supporting Information S1: Figure 2b). Representatively, the changing rate of most AAs maintained a dynamic equilibrium in the DO feast/famine cycle. Nonetheless, the changing rate of aspartate displayed a negative-positive-negative pattern, which was consistent with the changing pattern of extracellular DO as shown in Figure 2b. This implied that the DO perturbation might regulate the kinetics of intracellular aspartate, affecting its ability in AA biosynthesis. Notably, aspartate plays a pivotal role in alanine, threonine and arginine biosynthesis. In addition, the malate-aspartate shuttle system has an important effect on energy production. Consequently, a metabolic model with a dynamic metabolic profile, iAL1006D, was constructed to further investigate the adaptation mechanism of *P. chrysogenum* cells to such DO perturbation.

3.4.2 | Dynamic flux estimation by constraining the GEM model with time-resolved metabolite data

Based on the previous section, a dynamic changing rate analysis was performed on the measured 27 intracellular metabolites during the 150 s cycle. Then, their dynamic changing profiles were integrated into the GEM model of *P. chrysogenum* to construct the new model iAL1006D, which contains virtual dummy metabolic fluxes of 1652 reactions. Linear programming problems were set with the maximization of ATP maintenance as the objective to obtain the intracellular fluxes at each time point. Additionally, the measured dynamic metabolite data were represented by the mean value with the standard deviation as the upper and lower bounds when added to the model.

With metabolomics data of *P. chrysogenum* from periodic DO perturbation, fluxes of 1652 reactions were in silico predicted, of which fluxes of 889 reactions remained at zero. The enrichment analysis of KEGG pathways was performed on the 763 reactions with non-zero flux obtained during the periodic DO perturbation. The results are shown in Figure 8a. Based on the enrichment analysis result, periodic fluctuations in DO directly impact central carbon metabolic pathways. Particularly under hypoxic conditions, carbon flux is shifted towards pathways that demand less energy, such as the PP pathway. Many metabolites in central carbon metabolism are critical precursors for AA synthesis, so the synthesis of some AAs is significantly affected. For the penicillin biosynthesis pathway, the fluxes of AA precursors (valine, cysteine) decrease with DO concentration changes. Also, being sensitive to DO perturbations, energy metabolism and fatty acid metabolism show a significant change (Figure 8b). In the following sections, we mainly focused on the flux rearrangement in central carbon metabolism, AA metabolism, energy metabolism and fatty acid metabolism.

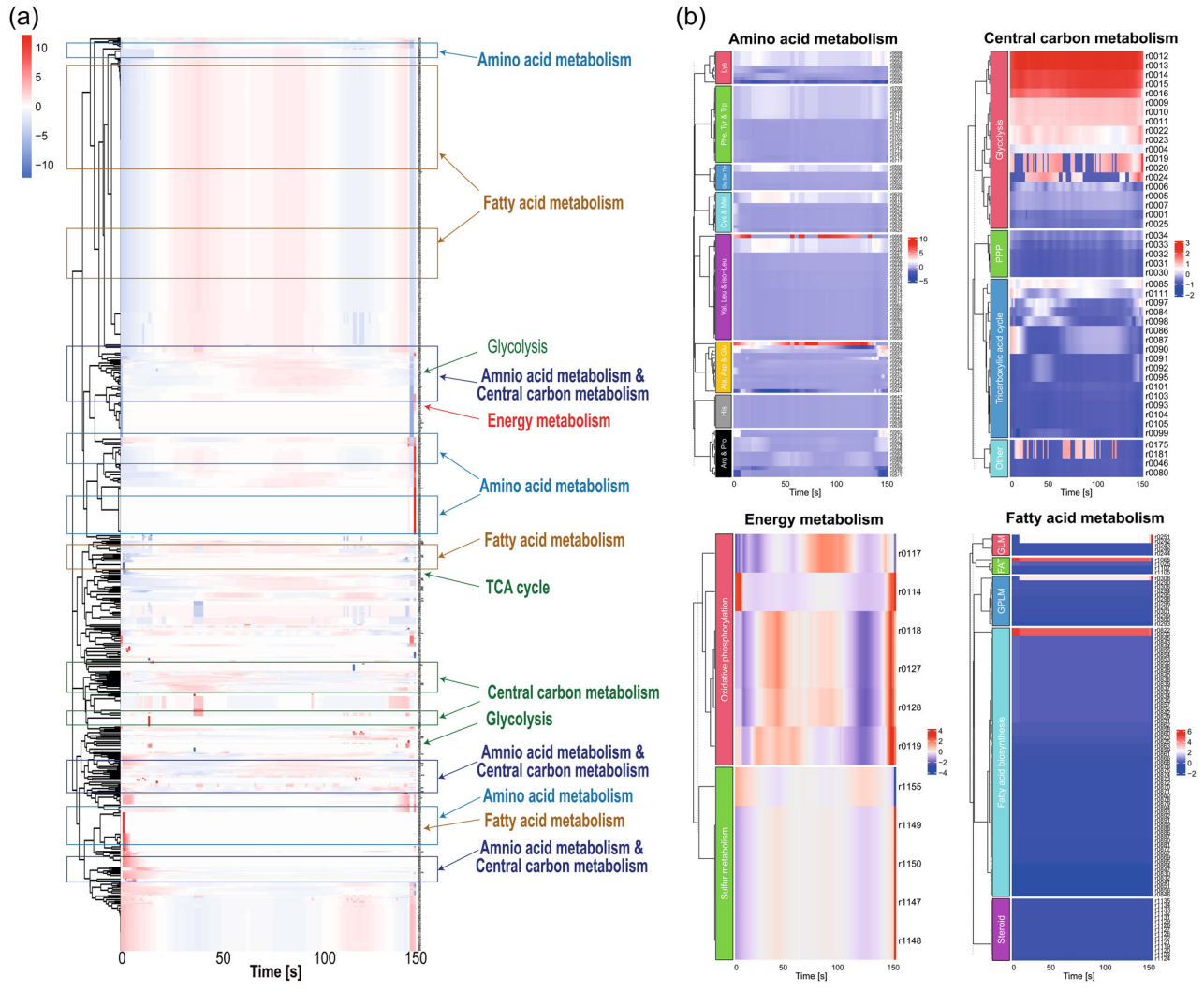

FIGURE 8 (a) The dynamic response of metabolic pathways in *Penicillium chrysogenum* during a DO feast/famine cycle. (b) The dynamic response in amino acids metabolic pathway, central carbon metabolic pathway, energy metabolic pathway and fatty acid metabolic pathway of *P. chrysogenum* under the DO oscillation cycle. DO, dissolved oxygen.

3.4.3 | Dynamic flux analysis of EMP pathway, TCA cycle and PP pathway under periodic DO perturbations

Figure 9 showed the distribution of dummy metabolic fluxes in the central carbon metabolic pathways of *P. chrysogenum* simulated by the new iAL1006D model. The changing pattern of the fluxes in the EMP pathway, TCA cycle, and PP pathways (Figure 9) was consistent with the trend of OUR in different stages over time (Figure 2d). The trend in the central carbon metabolism implied that the metabolites were withdrawn for anabolic purposes at high oxygen concentration, while the fluxes were enriched for cell growth at low oxygen concentration as shown in Figure 2b and Figure 9. For example, the fluxes of the EMP pathway increased smoothly and reached the peak at ~80 s. In contrast, the fluxes in the TCA cycle increased in the early stage (~40 s) and then ramped down. Despite the TCA cycle having been acknowledged as the most important pathway for the energy supply, it also plays a vital role in AA biosynthesis and the regulation of cellular redox state (Eniafe & Jiang, 2021; Fernie et al., 2004). The changing pattern demonstrated that when the DO concentration was high, the fluxes leading to the TCA cycle were increased. In contrast to the decline of fluxes of other reactions in the TCA cycle as the DO concentration was low, the fluxes of the reactions leading to the formation of malate and oxaloacetate were increased in the early 50 s, and then ramped down. Despite the important role of oxaloacetate and malate as key intermediates for anaplerotic purposes (van Gulik et al., 2000), they also participate into the malate/oxaloacetate shuttle system, involving the regeneration of NAD^+ in the cytosol and at the same time transferring NADH to the mitochondria. Hence, the aforementioned flux change indicates there may be an enhanced activity of malate/oxaloacetate shuttle system, which might contribute to maintaining the cellular redox balance (Al-Saryi et al., 2017).

The fluxes of PP pathway through the key metabolic nodes of G6P and fructose 6-phosphate (F6P) increased gradually as the DO concentration decreased. As the first branching point in central carbon metabolism, G6P, plays an important role in glycolysis, PP

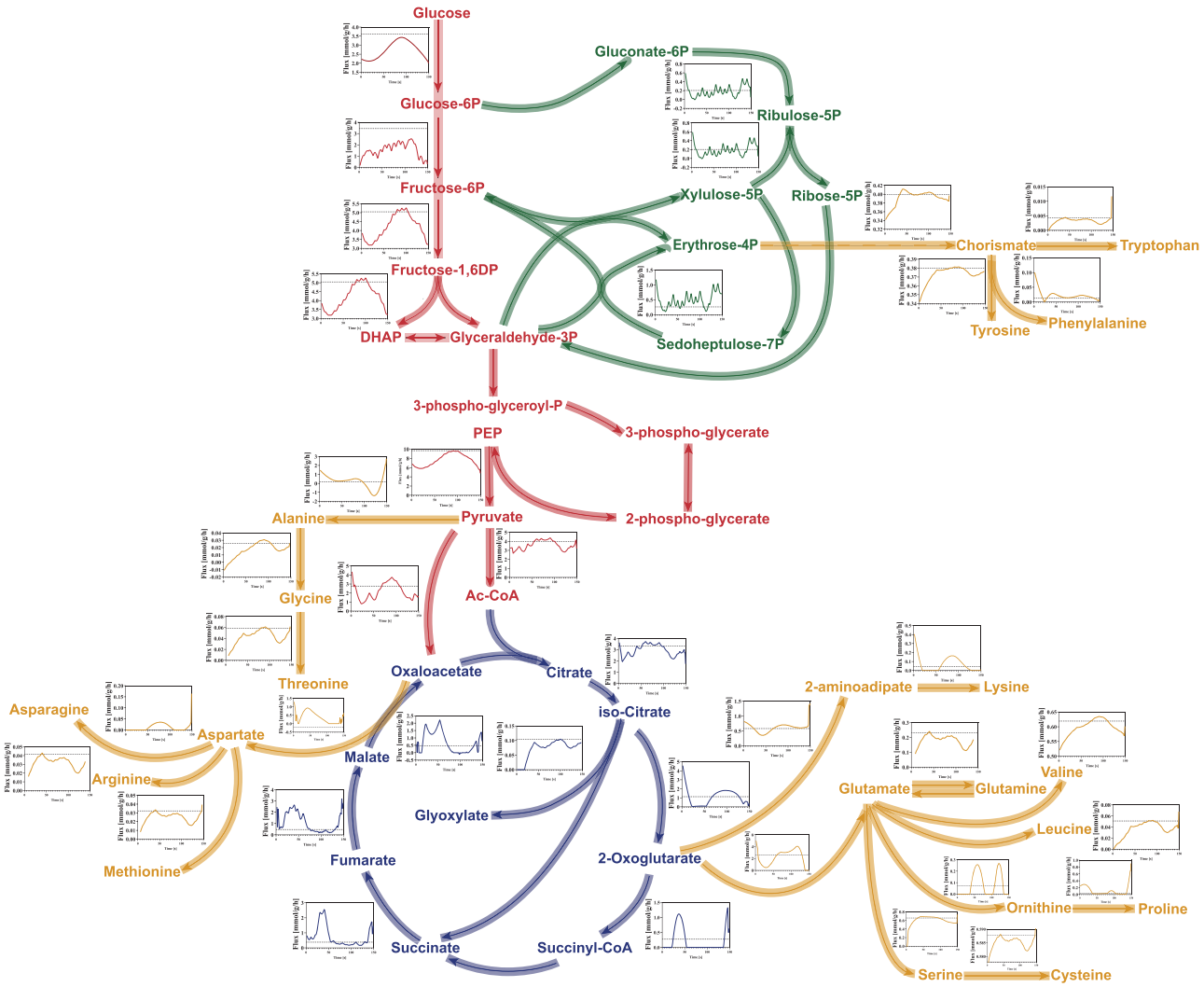

FIGURE 9 Simulated dynamic flux profiles of the central carbon metabolic pathway and amino acid metabolism of *Penicillium chrysogenum* under the DO oscillation cycle (colored line) and the DO steady state (dashed line). DO, dissolved oxygen.

pathway, and storage carbohydrate biosynthesis (Suarez-Mendez et al., 2017). In our experiments, 95% of the synthesized G6P was directed to glycolysis, and the remaining was left for the trehalose production. It has been well documented that trehalose facilitates the maintenance of a metabolically balanced state although the formation and degradation of trehalose will cause extra ATP costs (Wang et al., 2019, 2021). The trend of fluxes of trehalose production was similar to the trend of flux in EMP pathway, which implied that there might be a large increase in maintenance requirements under the DO oscillating condition. The second branching point in central carbon metabolism, F6P, plays an important role in the PP pathway, mannose and fructose metabolic pathway. In our experiments, 7% of synthesized F6P was directed to PP pathway. In PP pathway, the fluxes of production of sedoheptulose-7-phosphate (Sed7P) and erythrose-4-phosphate (E4P) increased gradually during the DO oscillating condition. As is known, E4P is important for the biosynthesis of shikimate and the derived aromatic AAs (Tran et al., 2011). Thus, the changing rate of phenylalanine (Supporting Information S1: Figure S2b) was consistent with the flux of E4P production (Figure 9). Additionally, we also observed an oscillating flux of the interconversion between fructose and mannitol under the DO oscillating condition (Supporting Information S1: Figure S3). It seems reasonable that these metabolites are sinks of reducing equivalents, thus potentially regulating the ratios of NADPH/$NADP^+$ and NADH/NAD^+ to maintain cellular redox balance under such dynamic DO conditions (Solomon et al., 2007).

3.4.4 | Dynamic flux analysis of energy metabolism, AA metabolism, and fatty acid biosynthesis under periodic DO perturbations

There were significant changes in the fluxes related to energy metabolic pathways, such as oxidative phosphorylation as shown in Figure 8. The interconversions of NAD(H) and FAD(H_2), and the generation of ATP reflected how cells responded to the environmental stress. To maintain an adequate intracellular ATP level, cells increased the fluxes of the conversion from NADH and $FADH_2$ to NAD^+ and FAD^+, respectively. Hence, the rate of proton gradient formation and ATP synthesis was increased. As the DO concentration increased, the increased production of ATP can meet increased energy demands to sustain essential cellular processes and maintain cell growth. In contrast, the flux of ATP-consuming reactions in the central carbon metabolic pathways was lower under high DO concentrations and gradually increased as DO decreased (Supporting Information S1: Figure 4). This period can be roughly divided into two stages, a high DO stage from 0 to 30 s and a mid-low DO stage from 30 to 150 s. The flux of ATP consumption during the mid-low DO stage is 1.89 times higher than that during the high DO stage. The limited ATP is preferentially allocated to support cell growth, thereby limiting its availability for penicillin production. In the penicillin synthesis, the IPNS catalyzing ACV into IPN requires oxygen as the co-substrate and also consumes ATP. The decreasing availability of ATP and oxygen in principle downregulates the catalytic capabilities of IPNS, leading to the reduction in penicillin productivity (de Jonge et al., 2011). Additionally, Henriksen et al. also observed that a reduction of DO concentration led to a decrease in the intracellular level of CoA−thioester-activated side-chain precursor, thereby aggravating the decrease in penicillin production capability (Henriksen et al., 1997). Besides this, AAs metabolism and fatty acid metabolism, which were associated with energy metabolism, also exhibited adaptive responses to changes in DO concentrations.

Figure 9 and Supporting Information S1: Figure S2b showed the dynamic flux distribution of AA metabolic pathways. The flux patterns of most AAs were consistent with the DO oscillation cycle. For example, the fluxes of valine, cysteine and leucine increased gradually as the DO concentration increased in the early stage, then levelled off and finally decreased at the low DO concentration. AAs played their roles in energy metabolic pathways as well as penicillin production. For example, cysteine and valine are crucial precursor AAs for penicillin biosynthesis. Under the DO oscillating condition, more energy and resources were most likely conserved to adapt to the new environment, leading to the decline of intracellular amount of both cysteine and valine, which might have a negative effect on the penicillin production (Douma et al., 2011; Janoska et al., 2022). Additionally, the flux of oxaloacetate to aspartate decreased when the DO concentration decreased, and even the flux was completely reversed to produce glutamate with the lowest DO concentration. Aspartate is crucial for nitrogen metabolism in *P. chrysogenum*. Under the low DO concentration, decreasing the flux of aspartate synthesis may result in the limitation of nitrogen for cell growth and other AAs production. As shown in Supporting Information S1: Figure 2b, the changing rates of alanine, leucine and isoleucine decreased as the rate of aspartate decreased. Another significant role of aspartate was to resist oxidative stress by regulating the intracellular NADPH and NADH level (Alhasawi et al., 2015; Lemire et al., 2017).

In addition, it is interesting to note that the fatty acid biosynthetic pathways were enriched as shown in Figure 8, and the flux change exhibited the similar trend to that of central carbon metabolism. When the DO declined, the flux of fatty acid biosynthetic pathway gradually decreased while the flux of the glyoxylate shunt increased, leading to maintenance of cellular redox balance under hypoxic conditions (Lu et al., 2018; Yang et al., 2022). Due to a significant amount of NADPH consumption for fatty acid biosynthesis, the decreased flux of this pathway could be a regulatory mechanism to mitigate excessive NADPH loss. Furthermore, fatty acids are essential building blocks of cell membranes and play a critical role in the transport of molecules across cell membranes, facilitating the exchange of substances between the intracellular and extracellular environments. Under the low DO condition, the cells may also adjust the fatty acid composition and structure of cell wall and membrane to regulate signal transduction, substrate/product transportation as well as energy supply (Degreif et al., 2017).

3.5 | Implications for large-scale fermentation

Induced by nonideal mixing and mass transfer limitations, gradients of substrate, DO, pH, dissolved CO_2 have inevitably occurred during bioreactor scale-up. Under this circumstance, microbes need to finely rearrange their metabolism to cope with such environmental gradients when traveling through different zones of large-scale bioreactors. To the best of our knowledge, most of previous studies have dealt with the investigation of the effect of substrate gradients on biomass growth and production performance. During penicillin production, oxygen is not only used as the electron acceptor on the respiration chain, but also required as the essential substrate for isopenicillin N synthetase catalyzing the second reaction for penicillin biosynthesis. To shed light on the effect of DO gradients on the metabolic response of *P. chrysogenum*, in our scale-down experiments, the cellular environment was characterized by periodic DO oscillations, repeatedly oscillating between high and low levels at the timescales comparable to the mixing time of an industrial-scale fermentor (>190 m^3). In large-scale bioreactors, however, the cells experience such oscillatory DO condition depending on the circulation flows, which is as a rule of thumb four times shorter than the mixing time. This was, indeed, a prerequisite for a rational cell lifeline-based scale-down and thus for a more proper evaluation of the metabolic response of the cells. Hence, whether the observed metabolic effects would be similar at shorter timescales close to the global circulation time should be further studied.

If cells in such non-ideally mixed industrial bioreactors suffer from DO gradients, drastic changes in both metabolite level and flux distribution at the expense of extra ATP and the deterioration of enzymes are indeed a cause for a lower productivity as argued above. To address this issue, a higher affinity system for oxygen can be engineered, for example, via heterologous expression of a bacterial hemoglobin to improve the growth and production properties of *P. chrysogenum*. More specifically, the IPNS might be engineered to increase the affinity for oxygen so that it becomes less sensitive to industrial-scale relevant DO changes. Despite the impaired penicillin productivity, it is interesting to note that the byproduct o-OH-PAA was less accumulated, probably caused by lower levels of enzymes PAA 2-hydroxylase activity under the oscillating DO condition. Based on these aforementioned findings, more elaborate scale-down experiments should be performed to determine the threshold of DO oscillations including both frequency and magnitude between low DO and high DO levels, which would have only a minor impact on cell growth and production performance. By doing so, these scale-down results can indeed provide important clues for bioreactor design and scale-up procedures as well as for constructing robust cell strains to cope with heterogenous industrial culture conditions.

4 | CONCLUSION

In this work, we proposed a DO scale-down setup that applies a block-wise nitrogen/oxygen switching regime in the gas inlet of glucose-limited chemostat cultures to simulate periodic DO perturbations for the evaluation of *P. chrysogenum* cell performance under conditions relevant to those encountered in large-scale practices. The scale-down results presented in this study showed that DO feast/famine conditions in large-scale bioreactors can lead to the reduced biomass yield and cause a considerable loss of penicillin productivity, which is accompanied by drastic changes in both metabolite level and flux rearrangement. Most prominent flux redistribution lies in central carbon metabolism, AA metabolism, energy metabolism and fatty acid metabolism. Economically, the precursor PAA was neither catabolized as the extra carbon source nor converted to the nonrecyclable byproduct o-OH-PAA but more directed towards penicillin production under the DO oscillating condition. Most interestingly, a steady extracellular glucose concentration and DO concentration may contribute to stabilizing cellular metabolic activities, maintaining the penicillin productivity and mitigating degeneration of penicillin production. Furthermore, dynamic flux profiles indicated that cellular metabolism of *P. chrysogenum* was efficiently rearranged among which metabolic pathways such as central carbon metabolism, AA metabolism, energy metabolism and fatty acid metabolism were most sensitively synchronized with the DO oscillation.

ACKNOWLEDGMENTS

This research was funded by the National Key R&D Program of China (Grant no. 2021YFC2101000), National Natural Science Foundation of China (Grant no. 31900073, 21978085), Shanghai Rising-Star Program (Grant no. 21QA1402400), Natural Science Foundation of Shanghai (Grant no. 19ZR1413600) and the Fundamental Research Funds for the Central Universities (Grant No. JKF01221709).

DATA AVAILABILITY STATEMENT

All data and code for this article can be found in https://github.com/ariel317/Dynamic-metabolic-flux-analysis-under-DO-oscillation-condition.

ORCID

Cees Haringa http://orcid.org/0000-0003-0310-1045
Ju Chu http://orcid.org/0000-0002-6406-1748
Guan Wang http://orcid.org/0000-0003-2341-3054

REFERENCES

Agren, R., Liu, L., Shoaie, S., Vongsangnak, W., Nookaew, I., & Nielsen, J. (2013). The RAVEN toolbox and its use for generating a genome-scale metabolic model for *Penicillium chrysogenum*. *PLoS Computational Biology*, *9*(3), e1002980. https://doi.org/10.1371/journal.pcbi.1002980

Alhasawi, A., Leblanc, M., Appanna, N. D., Auger, C., & Appanna, V. D. (2015). Aspartate metabolism and pyruvate homeostasis triggered by oxidative stress in *Pseudomonas fluorescens*: a functional metabolomic study. *Metabolomics*, *11*(6), 1792–1801. https://doi.org/10.1007/s11306-015-0841-4

Al-Saryi, N. A., Al-Hejjaj, M. Y., van Roermund, C. W. T., Hulmes, G. E., Ekal, L., Payton, C., Wanders, R. J. A., & Hettema, E. H. (2017). Two NAD-linked redox shuttles maintain the peroxisomal redox balance in *Saccharomyces cerevisiae*. *Scientific Reports*, *7*(1), 11868. https://doi.org/10.1038/s41598-017-11942-2

Anane, E., Knudsen, I. M., & Wilson, G. C. (2021). Scale-down cultivation in mammalian cell bioreactors—The effect of bioreactor mixing time on the response of CHO cells to dissolved oxygen gradients. *Biochemical Engineering Journal*, *166*, 107870. https://doi.org/10.1016/j.bej.2020.107870

Bhargava, S., Nandakumar, M. P., Roy, A., Wenger, K. S., & Marten, M. R. (2003). Pulsed feeding during fed-batch fungal fermentation leads to reduced viscosity without detrimentally affecting protein expression. *Biotechnology and Bioengineering*, *81*(3), 341–347. https://doi.org/10.1002/Bit.10481

Bhargava, S., Wenger, K. S., & Marten, M. R. (2003a). Pulsed addition of limiting-carbon during *Aspergillus oryzae* fermentation leads to improved productivity of a recombinant enzyme. *Biotechnology and Bioengineering*, *82*(1), 111–117. https://doi.org/10.1002/bit.10548

Bhargava, S., Wenger, K. S., & Marten, M. R. (2003b). Pulsed feeding during fed-batch *Aspergillus oryzae* fermentation leads to improved oxygen mass transfer. *Biotechnology Progress*, *19*(3), 1091–1094. https://doi.org/10.1021/Bp025694p

Canelas, A. B., van Gulik, W. M., & Heijnen, J. J. (2008). Determination of the cytosolic free NAD/NADH ratio in *Saccharomyces cerevisiae* under steady-state and highly dynamic conditions. *Biotechnology and Bioengineering*, *100*(4), 734–743. https://doi.org/10.1002/bit.21813

Degreif, D., de Rond, T., Bertl, A., Keasling, J. D., & Budin, I. (2017). Lipid engineering reveals regulatory roles for membrane fluidity in yeast flocculation and oxygen-limited growth. *Metabolic Engineering*, *41*, 46–56. https://doi.org/10.1016/j.ymben.2017.03.002

Deshmukh, A. T., Verheijen, P. J. T., Maleki Seifar, R., Heijnen, J. J., & van Gulik, W. M. (2015). In vivo kinetic analysis of the penicillin biosynthesis pathway using PAA stimulus response experiments. *Metabolic Engineering*, *32*, 155–173. https://doi.org/10.1016/j.ymben.2015.09.018

Diano, A., Bekker-Jensen, S., Dynesen, J., & Nielsen, J. (2006). Polyol synthesis in *Aspergillus niger*: Influence of oxygen availability, carbon and nitrogen sources on the metabolism. *Biotechnology and Bioengineering*, *94*(5), 899–908. https://doi.org/10.1002/bit.20915

Douma, R. D., Batista, J. M., Touw, K. M., Kiel, J. A., Krikken, A. M., Zhao, Z., Veiga, T., Klaassen, P., Bovenberg, R. A., Daran, J. M., Heijnen, J. J., & van Gulik, W. M. (2011). Degeneration of penicillin production in ethanol-limited chemostat cultivations of *Penicillium chrysogenum*: A systems biology approach. *BMC Systems Biology*, *5*, 132. https://doi.org/10.1186/1752-0509-5-132

Douma, R. D., Deshmukh, A. T., de Jonge, L. P., de Jong, B. W., Seifar, R. M., Heijnen, J. J., & van Gulik, W. M. (2012). Novel insights in transport mechanisms and kinetics of phenylacetic acid and penicillin-G in *Penicillium chrysogenum*. *Biotechnology Progress*, *28*(2), 337–348. https://doi.org/10.1002/btpr.1503

Douma, R. D., Verheijen, P. J. T., de Laat, W. T. A. M., Heijnen, J. J., & van Gulik, W. M. (2010). Dynamic gene expression regulation model for growth and penicillin production in *Penicillium chrysogenum*. *Biotechnology and Bioengineering*, *106*(4), 608–618. https://doi.org/10.1002/bit.22689

Eniafe, J., & Jiang, S. (2021). The functional roles of TCA cycle metabolites in cancer. *Oncogene*, *40*(19), 3351–3363. https://doi.org/10.1038/s41388-020-01639-8

Eriksen, S. H., Søderblom, T. B., Jensen, B., & Olsen, J. (1998). Uptake of phenylacetic acid by two strains of *Penicillium chrysogenum*. *Biotechnology and Bioengineering*, *60*(3), 310–316. https://doi.org/10.1002/(SICI)1097-0290(19981105)60:3<310::AID-BIT6>3.0.CO;2-K

Fernie, A. R., Carrari, F., & Sweetlove, L. J. (2004). Respiratory metabolism: glycolysis, the TCA cycle and mitochondrial electron transport. *Current Opinion in Plant Biology*, *7*(3), 254–261. https://doi.org/10.1016/j.pbi.2004.03.007

Garcia-Ochoa, F., & Gomez, E. (2009). Bioreactor scale-up and oxygen transfer rate in microbial processes: An overview. *Biotechnology Advances*, *27*(2), 153–176. https://doi.org/10.1016/j.biotechadv.2008.10.006

Garcia-Ortega, X., Valero, F., & Montesinos-Seguí, J. L. (2017). Physiological state as transferable operating criterion to improve recombinant protein production in *Pichia pastoris* through oxygen limitation. *Journal of Chemical Technology & Biotechnology*, *92*(10), 2573–2582. https://doi.org/10.1002/jctb.5272

Giles, N. M., Watts, A. B., Giles, G. I., Fry, F. H., Littlechild, J. A., & Jacob, C. (2003). Metal and Redox Modulation of cysteine protein function. *Chemistry & Biology*, *10*(8), 677–693. https://doi.org/10.1016/s1074-5521(03)00174-1

Goldrick, S., Ştefan, A., Lovett, D., Montague, G., & Lennox, B. (2015). The development of an industrial-scale fed-batch fermentation simulation. *Journal of Biotechnology*, *193*, 70–82. https://doi.org/10.1016/j.jbiotec.2014.10.029

Groen, D. J. (1994). Macromixing in bioreactors. *Delft University of Technology: Delft, The Netherlands*. http://resolver.tudelft.nl/uuid:3ac019f1-d19a-4853-9a29-554f1149bd5b

van Gulik, W. M., Antoniewicz, M. R., deLaat, W. T. A. M., Vinke, J. L., & Heijnen, J. J. (2001). Energetics of growth and penicillin production in a high-producing strain of *Penicillium chrysogenum*. *Biotechnology & Bioengineering*, *72*(2), 185–193. https://doi.org/10.1002/1097-0290(20000120)72:2<185::Aid-Bit7>3.0.Co;2-M

van Gulik, W. M., de Laat, W. T. A. M., Vinke, J. L., & Heijnen, J. J. (2000). Application of metabolic flux analysis for the identification of metabolic bottlenecks in the biosynthesis of penicillin-G. *Biotechnology and Bioengineering*, *68*(6), 602–618. https://doi.org/10.1002/(SICI)1097-0290(20000620)68:6<602::AID-BIT3>3.0.CO;2-2

Haringa, C., Tang, W., Deshmukh, A. T., Xia, J., Reuss, M., Heijnen, J. J., Mudde, R. F., & Noorman, H. J. (2016). Euler-Lagrange computational fluid dynamics for (bio)reactor scale down: An analysis of organism lifelines. *Engineering in Life Sciences*, *16*(7), 652–663. https://doi.org/10.1002/elsc.201600061

Henriksen, C. M., Nielsen, J., & Villadsen, J. (1997). Influence of the dissolved oxygen concentration on the penicillin biosynthetic pathway in Steady-State cultures of *Penicillium chrysogenum*. *Biotechnology Progress*, *13*(6), 776–782. https://doi.org/10.1021/bp970098u

Jaén, K. E., Sigala, J.-C., Olivares-Hernández, R., Niehaus, K., & Lara, A. R. (2017). Heterogeneous oxygen availability affects the titer and topology but not the fidelity of plasmid DNA produced by *Escherichia coli*. *BMC Biotechnology*, *17*(1), 60. https://doi.org/10.1186/s12896-017-0378-x

Jang, C., Chen, L., & Rabinowitz, J. D. (2018). Metabolomics and isotope tracing. *Cell*, *173*(4), 822–837. https://doi.org/10.1016/j.cell.2018.03.055

Janoska, A., Verheijen, J. J., Tang, W., Lee, Q., Sikkema, B., & van Gulik, W. M. (2022). Influence of oxygen concentration on the metabolism of *Penicillium chrysogenum*. *Engineering in Life Sciences*, *23*(1), e2100139. https://doi.org/10.1002/elsc.202100139

Jansen, M. L. A., Daran-Lapujade, P., de Winde, J. H., Piper, M. D. W., & Pronk, J. T. (2004). Prolonged maltose-limited cultivation of *Saccharomyces cerevisiae* selects for cells with improved maltose affinity and hypersensitivity. *Applied and Environmental Microbiology*, *70*(4), 1956–1963. https://doi.org/10.1128/Aem.70.4.1956-1963.2004

Jansen, M. L. A., Diderich, J. A., Mashego, M., Hassane, A., de Winde, J. H., Daran-Lapujade, P., & Pronk, J. T. (2005). Prolonged selection in aerobic, glucose-limited chemostat cultures of *Saccharomyces cerevisiae* causes a partial loss of glycolytic capacity. *Microbiology*, *151*(Pt 5), 1657–1669. https://doi.org/10.1099/mic.0.27577-0

Jansen, P., Slott, S., & Gurtler, H. (1978). Determination of mixing times in large scale fermentors using radioactive isotopes, *Proceedings of the 1st European Congress on Biotechnology* Part 2, Interlaken, (pp 80–82).

de Jonge, L., Buijs, N. A. A., Heijnen, J. J., van Gulik, W. M., Abate, A., & Wahl, S. A. (2014). Flux response of glycolysis and storage metabolism during rapid feast/famine conditions in *Penicillium chrysogenum* using dynamic13C labeling. *Biotechnology Journal*, *9*(3), 372–385. https://doi.org/10.1002/biot.201200260

de Jonge, L. P., Buijs, N. A. A., ten Pierick, A., Deshmukh, A., Zhao, Z., Kiel, J. A. K. W., Heijnen, J. J., & van Gulik, W. M. (2011). Scale-down of penicillin production in *Penicillium chrysogenum*. *Biotechnology Journal*, *6*(8), 944–958. https://doi.org/10.1002/biot.201000409

Kampers, L. F. C., Asin-Garcia, E., Schaap, P. J., Wagemakers, A., & Martins Dos Santos, V. A. P. (2021). From innovation to application: Bridging the valley of death in industrial biotechnology. *Trends in Biotechnology*, *39*(12), 1240–1242. https://doi.org/10.1016/j.tibtech.2021.04.010

Kleijn, R. J., Liu, F., van Winden, W. A., van Gulik, W. M., Ras, C., & Heijnen, J. J. (2007). Cytosolic NADPH metabolism in penicillin-G producing and non-producing chemostat cultures of *Penicillium chrysogenum*. *Metabolic Engineering*, *9*(1), 112–123. https://doi.org/10.1016/j.ymben.2006.08.004

Kuschel, M., & Takors, R. (2020). Simulated oxygen and glucose gradients as a prerequisite for predicting industrial scale performance a priori. *Biotechnology and Bioengineering*, *117*(9), 2760–2770. https://doi.org/10.1002/bit.27457

Lara, A. R., Galindo, E., Ramírez, O. T., & Palomares, L. A. (2006). Living with heterogeneities in bioreactors. *Molecular Biotechnology*, *34*(3), 355–382. https://doi.org/10.1385/MB:34:3:355

Lara, A. R., Leal, L., Flores, N., Gosset, G., Bolívar, F., & Ramírez, O. T. (2006). Transcriptional and metabolic response of recombinant *Escherichia coli* to spatial dissolved oxygen tension gradients simulated in a scale-down system. *Biotechnology and Bioengineering*, *93*(2), 372–385. https://doi.org/10.1002/bit.20704

Larsson, G., & Enfors, S. O. (1988). Studies of insufficient mixing in bioreactors: Effects of limiting oxygen concentrations and short term oxygen starvation on *Penicillium chrysogenum*. *Bioprocess engineering*, *3*(3), 123–127. https://doi.org/10.1007/BF00373475

Lemire, J., Alhasawi, A., Appanna, V. P., Tharmalingam, S., & Appanna, V. D. (2017). Metabolic defence against oxidative stress: the road less travelled so far. *Journal of Applied Microbiology*, *123*(4), 798–809. https://doi.org/10.1111/jam.13509

Li, C., Shu, W., Wang, S., Liu, P., Zhuang, Y., Zhang, S., & Xia, J. (2018). Dynamic metabolic response of *Aspergillus niger* to glucose perturbation: evidence of regulatory mechanism for reduced glucoamylase production. *Journal of Biotechnology*, *287*, 28–40. https://doi.org/10.1016/j.jbiotec.2018.08.005

Liu, P., Hua, Y., Zhang, W., Xie, T., Zhuang, Y., Xia, J., & Noorman, H. (2021). A new strategy for dynamic metabolic flux estimation by integrating transient metabolome data into genome-scale metabolic models. *Bioprocess and Biosystems Engineering*, *44*(12), 2553–2565. https://doi.org/10.1007/s00449-021-02626-3

Liu, P., Wang, S., Li, C., Zhuang, Y., Xia, J., & Noorman, H. (2021). Dynamic response of *Aspergillus niger* to periodical glucose pulse stimuli in chemostat cultures. *Biotechnology and Bioengineering*, *118*(6), 2265–2282. https://doi.org/10.1002/bit.27739

Liu, X., Sun, X., He, W., Tian, X., Zhuang, Y., & Chu, J. (2019). Dynamic changes of metabolomics and expression of candicidin biosynthesis gene cluster caused by the presence of a pleiotropic regulator AdpA in *Streptomyces ZYJ-6*. *Bioprocess and Biosystems Engineering*, *42*(8), 1353–1365. https://doi.org/10.1007/s00449-019-02135-4

Löffler, M., Simen, J. D., Jäger, G., Schäferhoff, K., Freund, A., & Takors, R. (2016). Engineering *E. coli* for large-scale production—Strategies considering ATP expenses and transcriptional responses. *Metabolic Engineering*, *38*, 73–85. https://doi.org/10.1016/j.ymben.2016.06.008

Lu, H., Cao, W., Liu, X., Sui, Y., Ouyang, L., Xia, J., Huang, M., Zhuang, Y., Zhang, S., Noorman, H., & Chu, J. (2018). Multi-omics integrative analysis with genome-scale metabolic model simulation reveals global cellular adaptation of *Aspergillus niger* under industrial enzyme production condition. *Scientific Reports*, *8*(1), 14404. https://doi.org/10.1038/s41598-018-32341-1

Mashego, M., Jansen, M., Vinke, J., van Gulik, W., & Heijnen, J. (2005). Changes in the metabolome of associated with evolution in aerobic glucose-limited chemostats. *FEMS Yeast Research*, *5*(4–5), 419–430. https://doi.org/10.1016/j.femsyr.2004.11.008

Nadal-Rey, G., McClure, D. D., Kavanagh, J. M., Cornelissen, S., Fletcher, D. F., & Gernaey, K. V. (2021). Understanding gradients in industrial bioreactors. *Biotechnology Advances*, *46*, 107660. https://doi.org/10.1016/j.biotechadv.2020.107660

Nasution, U., van Gulik, W. M., Kleijn, R. J., van Winden, W. A., Proell, A., & Heijnen, J. J. (2006). Measurement of intracellular metabolites of primary metabolism and adenine nucleotides in chemostat cultivated *Penicillium chrysogenum*. *Biotechnology and Bioengineering*, *94*(1), 159–166. https://doi.org/10.1002/bit.20842

Nasution, U., van Gulik, W. M., Proell, A., van Winden, W. A., & Heijnen, J. J. (2006). Generating short-term kinetic responses of primary metabolism of *Penicillium chrysogenum* through glucose perturbation in the bioscope mini reactor. *Metabolic Engineering*, *8*(5), 395–405. https://doi.org/10.1016/j.ymben.2006.04.002

Neubauer, P., & Junne, S. (2010). Scale-down simulators for metabolic analysis of large-scale bioprocesses. *Current Opinion in Biotechnology*, *21*(1), 114–121. https://doi.org/10.1016/j.copbio.2010.02.001

Neubauer, P., & Junne, S. (2016). Scale-up and scale-down methodologies for bioreactors. John Wiley & Sons. https://doi.org/10.1002/9783527683369.ch11

Paul, K., Böttinger, K., Mitic, B. M., Scherfler, G., Posch, C., Behrens, D., Huber, C. G., & Herwig, C. (2020). Development, characterization, and application of a 2-Compartment system to investigate the impact of pH inhomogeneities in large-scale CHO-based processes. *Engineering in Life Sciences*, *20*(8), 368–378. https://doi.org/10.1002/elsc.202000009

Pedersen, L., Hansen, K., Nielsen, J., Lantz, A. E., & Thykaer, J. (2012). Industrial glucoamylase fed-batch benefits from oxygen limitation and high osmolarity. *Biotechnology and Bioengineering*, *109*(1), 116–124. https://doi.org/10.1002/Bit.23287

Pollard, D. J., Kirschner, T. F., Hunt, G. R., Tong, I. T., Stieber, R., & Salmon, P. M. (2007). Scale up of a viscous fungal fermentation: Application of scale-up criteria with regime analysis and operating boundary conditions. *Biotechnology and Bioengineering*, *96*(2), 307–317. https://doi.org/10.1002/bit.21112

Revilla, G., Ramos, F. R., López-Nieto, M. J., Alvarez, E., & Martín, J. F. (1986). Glucose represses formation of delta-(L-alpha-aminoadipyl)-L-cysteinyl-D-valine and isopenicillin N synthase but not penicillin acyltransferase in *Penicillium chrysogenum*. *Journal of Bacteriology*, *168*(2), 947–952. https://doi.org/10.1128/jb.168.2.947-952.1986

Rodríguez-Sáiz, M., Barredo, J. L., Moreno, M. A., Fernández-Cañón, J. M., Peñalva, M. A., & Díez, B. (2001). Reduced function of a phenylacetate-oxidizing cytochrome p450 caused strong genetic improvement in early phylogeny of penicillin-producing strains. *Journal of Bacteriology*, *183*(19), 5465–5471. https://doi.org/10.1128/JB.183.19.5465-5471.2001

Simen, J. D., Löffler, M., Jäger, G., Schäferhoff, K., Freund, A., Matthes, J., Müller, J., & Takors, R. (2017). Transcriptional response of *Escherichia coli* to ammonia and glucose fluctuations. *Microbial*

Biotechnology, *10*(4), 858–872. https://doi.org/10.1111/1751-7915.12713

Solomon, P. S., Waters, O. D. C., & Oliver, R. P. (2007). Decoding the mannitol enigma in filamentous fungi. *Trends in Microbiology*, *15*(6), 257–262. https://doi.org/10.1016/j.tim.2007.04.002

Suarez-Mendez, C. A., Ras, C., & Wahl, S. A. (2017). Metabolic adjustment upon repetitive substrate perturbations using dynamic 13C-tracing in yeast. *Microbial Cell Factories*, *16*(1), 161. https://doi.org/10.1186/s12934-017-0778-6

Sweere, A. P. J., Mesters, J. R., Janse, L., Luyben, K. C. A. M., & Kossen, N. W. F. (1988). Experimental simulation of oxygen profiles and their influence on baker's yeast production: I. One-fermentor system. *Biotechnology and Bioengineering*, *31*(6), 567–578. https://doi.org/10.1002/bit.260310609

Takors, R. (2012). Scale-up of microbial processes: impacts, tools and open questions. *Journal of Biotechnology*, *160*(1–2), 3–9. https://doi.org/10.1016/j.jbiotec.2011.12.010

Teusink, B., Diderich, J. A., Westerhoff, H. V., van Dam, K., & Walsh, M. C. (1998). Intracellular glucose concentration in derepressed yeast cells consuming glucose is high enough to reduce the glucose transport rate by 50%. *Journal of Bacteriology*, *180*(3), 556–562. https://doi.org/10.1128/jb.180.3.556-562.1998

Theilgaard, H. B. A., Kristiansen, K. N., Henriksen, C. M., & Nielsen, J. (1997). Purification and characterization of δ-(L-α-aminoadipyl)-L-cysteinyl-D-valine synthetase from *Penicillium chrysogenum*. *Biochemical Journal*, *327*(1), 185–191. https://doi.org/10.1042/bj3270185

Thykaer, J., Rueksomtawin, K., Noorman, H., & Nielsen, J. (2008). NADPH-dependent glutamate dehydrogenase in *Penicillium chrysogenum* is involved in regulation of β-lactam production. *Microbiology*, *154*, 1242–1250.

Tran, D., Pietersma, A. L., Schofield, L. R., Rost, M., Jameson, G. B., & Parker, E. J. (2011). Investigating the role of the hydroxyl groups of substrate erythrose 4-phosphate in the reaction catalysed by the first enzyme of the shikimate pathway. *Bioorganic & Medicinal Chemistry Letters*, *21*(22), 6838–6841. https://doi.org/10.1016/j.bmcl.2011.09.017

Tsuge, Y., Uematsu, K., Yamamoto, S., Suda, M., Yukawa, H., & Inui, M. (2015). Glucose consumption rate critically depends on redox state in *Corynebacterium glutamicum* under oxygen deprivation. *Applied Microbiology and Biotechnology*, *99*(13), 5573–5582. https://doi.org/10.1007/s00253-015-6540-2

Vardar, F., & Lilly, M. D. (1982). Effect of cycling dissolved oxygen concentrations on product formation in penicillin fermentations. *European Journal of Applied Microbiology and Biotechnology*, *14*, 203–211. https://doi.org/10.1007/BF00498464

Vasilakou, E., van Loosdrecht, M. C. M., & Wahl, S. A. (2020). *Escherichia coli* metabolism under short-term repetitive substrate dynamics: adaptation and trade-offs. *Microbial Cell Factories*, *19*(1), 116. https://doi.org/10.1186/s12934-020-01379-0

Wang, G., Chu, J., Noorman, H., Xia, J., Tang, W., Zhuang, Y., & Zhang, S. (2014). Prelude to rational scale-up of penicillin production: A scale-down study. *Applied Microbiology and Biotechnology*, *98*(6), 2359–2369. https://doi.org/10.1007/s00253-013-5497-2

Wang, G., Chu, J., Zhuang, Y., van Gulik, W., & Noorman, H. (2019). A dynamic model-based preparation of uniformly-(13)C-labeled internal standards facilitates quantitative metabolomics analysis of *Penicillium chrysogenum*. *Journal of Biotechnology*, *299*, 21–31. https://doi.org/10.1016/j.jbiotec.2019.04.021

Wang, G., Haringa, C., Noorman, H., Chu, J., & Zhuang, Y. (2020). Developing a computational framework to advance bioprocess Scale-Up. *Trends in Biotechnology*, *38*(8), 846–856. https://doi.org/10.1016/j.tibtech.2020.01.009

Wang, G., Haringa, C., Tang, W., Noorman, H., Chu, J., Zhuang, Y., & Zhang, S. (2020). Coupled metabolic-hydrodynamic modeling enabling rational scale-up of industrial bioprocesses. *Biotechnology and Bioengineering*, *117*(3), 844–867. https://doi.org/10.1002/bit.27243

Wang, G., Tang, W., Xia, J., Chu, J., Noorman, H., & van Gulik, W. M. (2015). Integration of microbial kinetics and fluid dynamics toward model-driven scale-up of industrial bioprocesses. *Engineering in Life Sciences*, *15*(1), 20–29. https://doi.org/10.1002/elsc.201400172

Wang, G., Wang, X., Wang, T., van Gulik, W., Noorman, H. J., Zhuang, Y., Chu, J., & Zhang, S. (2019). Comparative fluxome and metabolome analysis of formate as an auxiliary substrate for penicillin production in Glucose-Limited cultivation of *Penicillium chrysogenum*. *Biotechnology Journal*, *14*(10), e1900009. https://doi.org/10.1002/biot.201900009

Wang, G., Wu, B., Zhao, J., Haringa, C., Xia, J., Chu, J., Zhuang, Y., Zhang, S., Heijnen, J. J., van Gulik, W., Deshmukh, A. T., & Noorman, H. J. (2018). Power input effects on degeneration in prolonged penicillin chemostat cultures: A systems analysis at flux, residual glucose, metabolite, and transcript levels. *Biotechnology and Bioengineering*, *115*(1), 114–125. https://doi.org/10.1002/bit.26447

Wang, G., Zhao, J., Haringa, C., Tang, W., Xia, J., Chu, J., Zhuang, Y., Zhang, S., Deshmukh, A. T., van Gulik, W., Heijnen, J. J., & Noorman, H. J. (2018). Comparative performance of different scale-down simulators of substrate gradients in *Penicillium chrysogenum* cultures: the need of a biological systems response analysis. *Microbial Biotechnology*, *11*(3), 486–497. https://doi.org/10.1111/1751-7915.13046

Wang, G., Zhao, J., Wang, X., Wang, T., Zhuang, Y., Chu, J., Zhang, S., & Noorman, H. J. (2019). Quantitative metabolomics and metabolic flux analysis reveal impact of altered trehalose metabolism on metabolic phenotypes of *Penicillium chrysogenum* in aerobic glucose-limited chemostats. *Biochemical Engineering Journal*, *146*, 41–51. https://doi.org/10.1016/j.bej.2019.03.006

Wang, X., Zhao, J., Xia, J., Wang, G., Chu, J., & Zhuang, Y. (2021). Impact of altered trehalose metabolism on physiological response of *Penicillium chrysogenum* chemostat cultures during industrially relevant rapid Feast/Famine conditions. *Processes*, *9*(1), 118. https://doi.org/10.3390/pr9010118

Weber, S. S., Polli, F., Boer, R., Bovenberg, R. A. L., & Driessen, A. J. M. (2012). Increased penicillin production in *Penicillium chrysogenum* production strains via balanced overexpression of isopenicillin N acyltransferase. *Applied and Environmental Microbiology*, *78*(19), 7107–7113. https://doi.org/10.1128/AEM.01529-12

White, R. L., John, E. M. M., Baldwin, J. E., & Abraham, E. P. (1982). Stoichiometry of oxygen consumption in the biosynthesis of isopenicillin from a tripeptide. *Biochemical Journal*, *203*(3), 791–793. https://doi.org/10.1042/bj2030791

Wu, L., Mashego, M. R., van Dam, J. C., Proell, A. M., Vinke, J. L., Ras, C., van Winden, W. A., van Gulik, W. M., & Heijnen, J. J. (2005). Quantitative analysis of the microbial metabolome by isotope dilution mass spectrometry using uniformly 13C-labeled cell extracts as internal standards. *Analytical Biochemistry*, *336*(2), 164–171. https://doi.org/10.1016/j.ab.2004.09.001

Yang, J. D., Lu, C., Stasny, B., Henley, J., Guinto, W., Gonzalez, C., Gleason, J., Fung, M., Collopy, B., Benjamino, M., Gangi, J., Hanson, M., & Ille, E. (2007). Fed-batch bioreactor process scale-up from 3-L to 2,500-L scale for monoclonal antibody production from cell culture. *Biotechnology and Bioengineering*, *98*(1), 141–154. https://doi.org/10.1002/bit.21413

Yang, Q., Lin, W., Xu, J., Guo, N., Zhao, J., Wang, G., Wang, Y., Chu, J., & Wang, G. (2022). Changes in oxygen availability during Glucose-Limited chemostat cultivations of *Penicillium chrysogenum* lead to rapid metabolite, flux and productivity responses. *Metabolites*, *12*(1), 45. https://doi.org/10.3390/metabo12010045

Zhao, Z., Ten Pierick, A., de Jonge, L., Heijnen, J. J., & Wahl, S. A. (2012). Substrate cycles in *Penicillium chrysogenum* quantified by isotopic non-stationary flux analysis. *Microbial Cell Factories*, *11*, 140. https://doi.org/10.1186/1475-2859-11-140

SUPPORTING INFORMATION

Additional supporting information can be found online in the Supporting Information section at the end of this article.

How to cite this article: Wang, X., Yang, Q., Haringa, C., Wang, Z., Chu, J., Zhuang, Y., & Wang, G. (2024). An industrial perspective on metabolic responses of *Penicillium chrysogenum* to periodic dissolved oxygen feast-famine cycles in a scale-down system. *Biotechnology and Bioengineering*, 1–23. https://doi.org/10.1002/bit.28782